Journal of Ecological Engineering Design

Modeling the Impact of Hydraulic Reconnection on Estuary Hydrodynamics

Megan Kramer[1] Mauricio Arias[1]

[1]University of South Florida, Tampa

American Ecological Engineering Society

Published on: Jun 05, 2023

URL: https://jeed.pubpub.org/pub/model-impact-hydraulic-reconnect

Abstract

Coastal environments around the globe are subject to anthropogenic stresses due to dense coastal populations. The response of development activities on dynamic estuarine ecosystems, influenced by tidal forces, freshwater flows, salinity variations, and intricate coastal land morphology, is often uncertain. This case study evaluates how connectivity and coastal geomorphology influence flow patterns by modeling the effects of a proposed hydraulic reconnection project on water movement between the Manchester Waterway, a coastal residential community, and Charlotte Harbor, a large open water estuary in the Gulf of Mexico. An unstructured grid, 2D model was developed utilizing Delft3D Flexible Mesh to simulate estuary hydrodynamics under proposed conditions for four different weather conditions, including recorded 2021–2022 weather, future sea level rise, an extreme weather event, and a combination of extreme weather and sea level rise. Simulated flow results for proposed conditions were compared to present day flow patterns for analysis of the predicted changes in water levels and velocity magnitudes in the waterway. The results show that increased connectivity between the Manchester Waterway and Charlotte Harbor is expected to increase tidal amplitudes largely due to a lowering of minimum water levels in the waterway. During storm events, water elevations are predicted to drop to lower elevations following peak storm surge due to proposed conditions, which may provide flooding relief. Model simulation results will aid hydraulic reconnection and guide a more comprehensive ecological restoration plan. This case study will also improve understanding of the major influencing forces in intricate estuarine environments and how ecosystems may respond to land development, sea level rise, and increasing magnitude and frequency of tropical storms.

Keywords Estuary; Coastal; Hydrodynamic modeling; Sea level rise; Tidal

1. Introduction

Over one-third of the global population is concentrated within 100 km from the coast, with some of the fastest growing megacities located next to deltas (Brown et al. 2013) and approximately 230 million people living in coastal areas below 1 m of high tide lines (Kulp and Strauss 2019). Coastal areas hold high economic and cultural value, because ports are important for international trade and transportation, fishing provides food for much of the world, and beaches are popular areas for recreation. This concentration of human development along coastlines has many serious implications for communities exposed to coastal hazards, including tropical storms, sea level rise, erosion, and harmful algal blooms. To reduce threats of erosion and property loss from coastal processes, massive development operations have been undertaken, which alter the natural shoreline. The installation of shoreline hardening structures, such as seawalls, riprap revetment, piers, and breakwaters, has helped make coastal regions habitable by serving as physical barriers between the land and sea. In many regions, the tragic consequence of these historic developments is coastal ecosystem decline. Hardened shorelines threaten species biodiversity in the littoral zone because they often replace or impair productive coastal habitats. Nearshore habitats are also threatened by human activities that alter watershed functions and

water quality (Prosser et al. 2018). In some cases, perimeter dikes have eliminated sediment supply to estuary marshes and reduced the tidal prism (Weishar et al. 2005). Increased dredging activities and reduced downstream sediment supply have further deteriorated the ecological value of many estuaries (Stark et al. 2017).

The degradation of estuarine habitats has prompted coastal ecosystem restoration projects worldwide for the benefit of both human communities and natural habitats. Such projects aim to restore ecological function through changes to land cover and environmental flows, following the estuarine ecohydrology concept that recognizes physics often drive the ecological and biological processes of a system (Wolanski and Elliot 2015). This can include the creation of intertidal wetlands, changes to water infrastructure to maintain freshwater flows, and dredging to improve water flow and residence time in stressed estuaries (Wolanski and Elliot 2015). These efforts are gaining popularity as sustainable approaches to regaining the ecosystem services provided by estuaries (Stark et al. 2017).

Technological advancements in recent decades have provided tools for predicting outcomes of coastal restoration efforts. Numerical modeling has been applied in several case studies for simulating biological and/or hydrodynamic responses to changes in estuary morphology and flow regimes (George et al. 2012; Stark et al. 2017; Wan et al. 2012; Weishar et al. 2005). Some consequences of modifications to geomorphology can involve an array of physical changes including altered flood patterns, water circulation, salinity and temperature distribution, sediment transport, tidal prism, and tidal asymmetry (Stark et al. 2017).

This study utilizes a proposed hydraulic reconnection project in Charlotte Harbor, Florida, as a case study to investigate how restoration of coastal geomorphology influences flow patterns in an intricate estuarine ecosystem. The main objective of this project was to quantify how the proposed reconnections would alter estuarine hydrodynamics under a range of extreme future scenarios. For the purpose of this study, the effects of the proposed project on water movement between the Manchester Waterway and Charlotte Harbor were simulated, focusing specifically on two fundamental indicators: surface water elevations and velocity. Given that sea level rise is likely to alter estuarine flows, we considered both short-term and long-term impacts of the proposed hydraulic reconnection. Short-term impacts were considered by evaluating hydrodynamics of the waterway under recorded 2021–2022 weather conditions and during a storm event. Long-term impacts were considered by evaluating the waterway under future sea-level-rise projections, and future storm events in combination with sea-level-rise.

2. Case Study Site

The growing Manchester Waterway community located in Port Charlotte, Florida (Fig. 1), is interested in improving boat access by restoring previous connections between the local waterway and the harbor, separated by a mangrove vegetated barrier peninsula. As the community continues to develop along the waterway, there is increasing motivation to reduce navigation time through slow no-wake zones to the harbor, reduce boat

traffic through the sole access channel, improve emergency response time, provide better waterway flushing, and provide additional recreational opportunities to paddlers. This endeavor has prompted an investigation into alternative navigational routes between the residential waterway and the harbor, for which 3 harbor connections, designed to connect the west and southwest portions of the Manchester Waterway community to the harbor, have been proposed (Fig. 1). Each connection would be formed by dredging three, 12-meter-wide channels through the existing barrier peninsula vegetated with mangrove, pine palmetto flatwoods, and Juncus marshes, currently protected as part of Charlotte Harbor Preserve State Park. It is known that the geometry, distribution, and size of inlets through barrier islands influence the volume of water transferred to semienclosed back-barrier bays, with larger inlets allowing for greater tidal range (Aretxabaleta et al. 2014). Thus, prior to the implementation of these reconnection plans, we find it critical to evaluate the impacts that such changes may have on local water circulation, for there is concern that restoring hydraulic connections through the barrier peninsula would increase flooding to homes near the proposed connections during storm events, as well as concern about the ecological impacts associated with the proposed changes. Innovative methods of assessing high-resolution estuary hydrodynamics are needed in order to characterize changes to local flow trends.

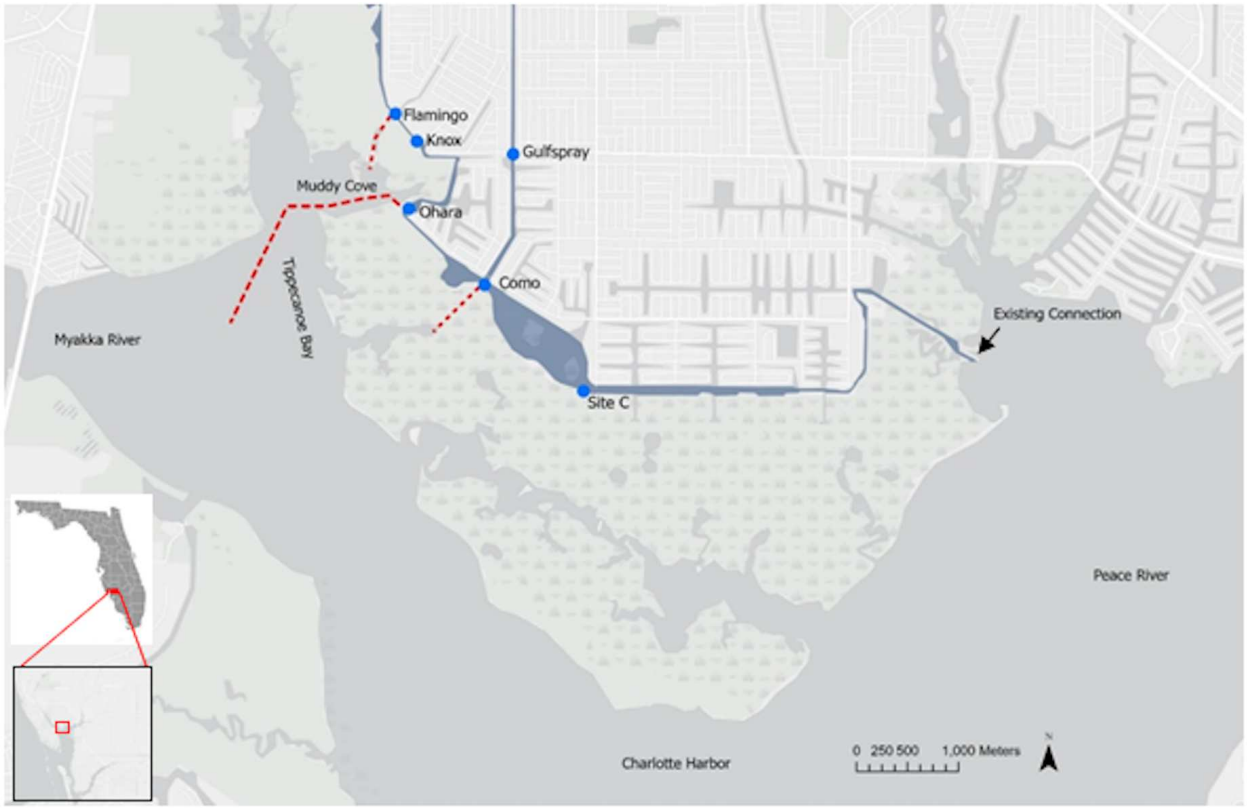

Fig. 1. Map of Manchester Waterway (shaded in blue) and 3 proposed connections (red dashed lines), with analysis sites indicated by blue circles. (Map created using ArcGIS 2.7.0 software by Esri. ArcGIS is the intellectual property of Esri and is used herein under license.)

Charlotte Harbor is located between Sarasota and Fort Myers on the Gulf Coast of Florida, United States of America, and is recognized as the second-largest estuary in Florida, serving as home to diverse wildlife where salt water from the Gulf of Mexico mixes with fresh water from the Myakka, Peace, and Caloosahatchee rivers (FDEP 2021). The harbor open-water surface area covers approximately 700 km^2, averages just over 2 m deep (FDEP 2005), and is largely bordered by Florida's third largest state park, Charlotte Harbor Preserve State Park, which protects over 160 km of shoreline and 183 km^2 of land (Florida State Parks 2022). This region is characterized by mixed semidiurnal tides.

Prior to development, the Manchester Waterway area in Charlotte Harbor consisted of meandering tidal creeks through pine and palmetto flatwoods (Fig. 2a). In the late 1950s through early 1960s, the area was excavated to create canals and fill for development (Fig. 2b). A lock was constructed in 1975 to provide residents access to Charlotte Harbor. Following permitting in 1977 that allowed additional residential development, navigational access was reduced when connections in the upper Manchester Waterway were plugged during construction and development (Fig. 2c; Manchester Waterway Civic Association 2021). The lock was removed in 2007 to address environmental concerns, and the channel to the east of the waterway remains the only navigational channel between the Manchester Waterway and the harbor (Fig. 1).

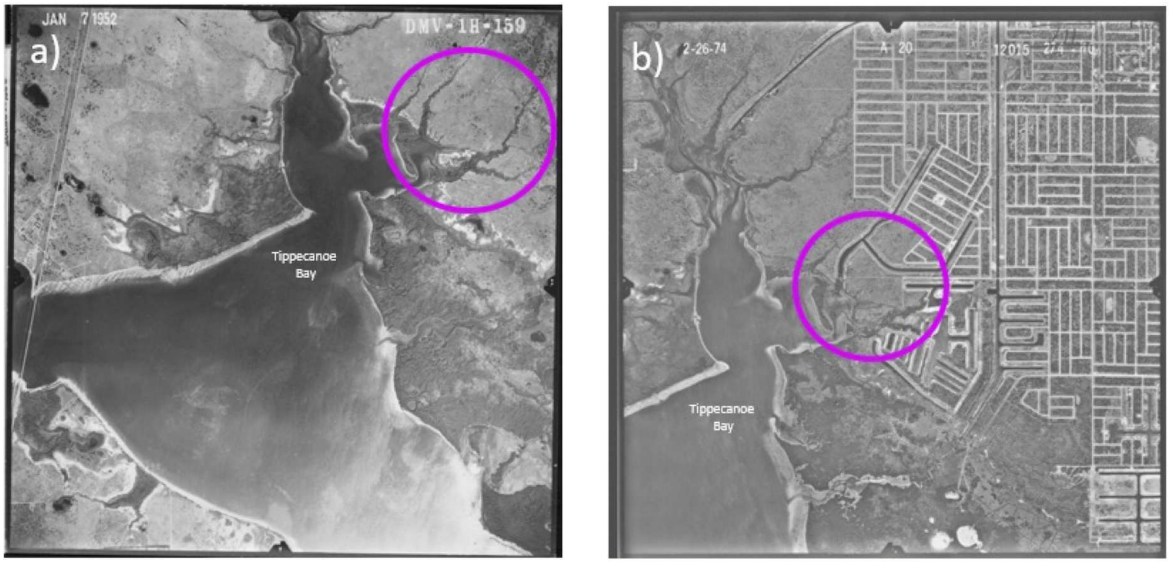

Fig. 2. Historical images of Manchester Waterway. a) 1952 image showing natural tidal creeks circled (USDA 1952), b) 1974 image of development in Manchester Waterway with connection between Tippecanoe Bay and the waterway circled (USDA 1974), (c) 2022 image of present-day conditions in the waterway, showing fill between previous connection to Tippecanoe Bay circled (Google Earth Pro 2022).

Water movement in Charlotte Harbor has been evaluated in several previous modeling studies. A three-dimensional water quality modeling system was developed by Kim et al. (2010) to forecast hypoxia in the upper harbor. Chen (2020) further investigated salinity transport processes and thermodynamics in the region using a coupled 3D–2D (laterally averaged) model with a domain that incorporated the major contributing rivers. The response of the harbor to Hurricane Irma was evaluated with the West Florida Coastal Ocean Model, which simulated the observed negative surge and corresponding drying of the estuary and Tampa Bay (Liu et al. 2020). The estuary and gulf circulation patterns were also assessed in a three-dimensional modeling study, which evaluated the influence of tides, rivers, and wind on estuarine hydrodynamics and salinity (Zheng and Weisberg 2004). These models extend from the tidal rivers to the Gulf of Mexico, providing information on regional water movement, without predicting hydrodynamic behavior in the narrow inland channels. In this study we used a high spatial-resolution model to extend understanding of this estuary into a residential waterway. We worked closely with community members to learn about the system, collect data, and understand their navigational concerns.

3. Methods

3.1 Model Description

Changes to water movement were investigated by simulating two-dimensional, depth-averaged, unsteady flow with the open-source modeling suite, Delft3D Flexible Mesh. This numerical hydrodynamic modeling software solves the equations of motion, the continuity equation, and the transport equations for conservative constituents. An orthogonal unstructured grid with Cartesian coordinates (Fig. 3) was developed to solve the Navier Stokes equations for incompressible fluid under the shallow water and Boussinesq assumptions (Deltares 2021). The model domain extends from the lower Peace and Myakka rivers toward the Gulf of Mexico to mid-Charlotte Harbor. The entire grid consists of 63,868 nodes, with grid lengths varying from approximately 300 m at the open boundaries to 15 m within the channels of the Manchester Waterway.

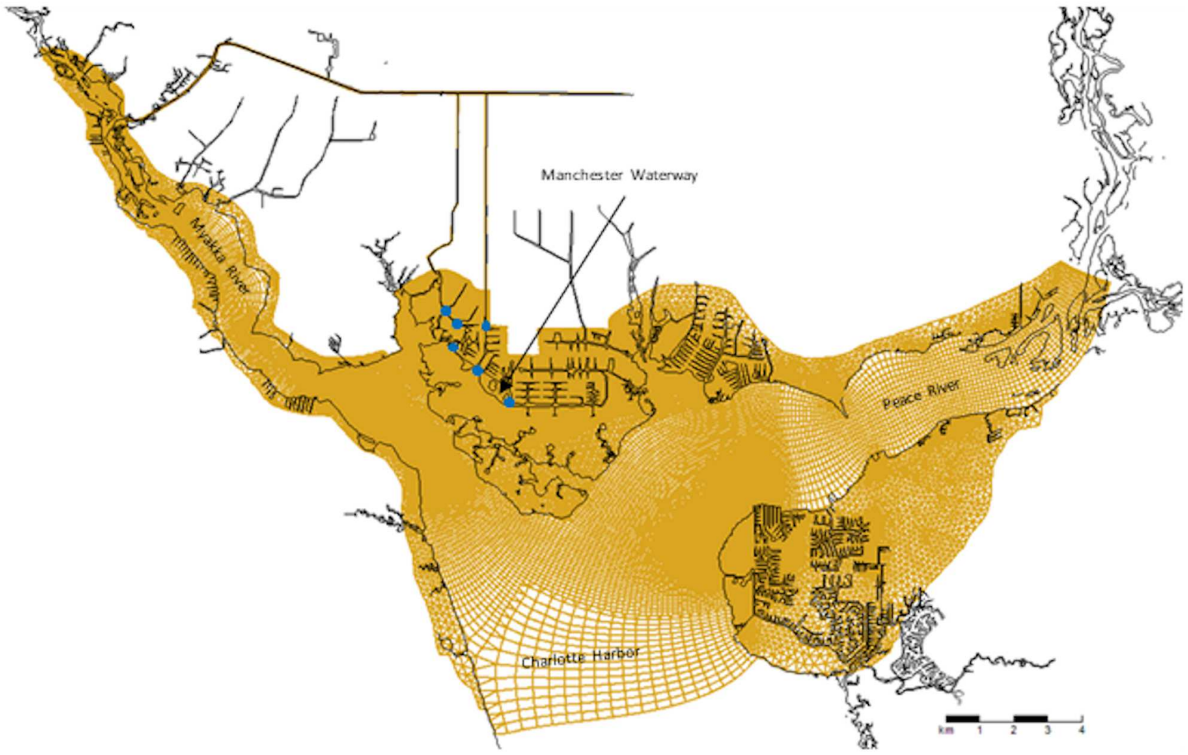

Fig. 3. Unstructured mesh developed for Delft3D hydrodynamic modeling of the Manchester Waterway, extending from Charlotte Harbor to the lower Myakka and Peace rivers. Analysis sites are indicated by blue circles. (Map created using Deltares D-Flow FM module.)

A synthesis of all datasets used for this model is presented in the Supplementary Material (Table S2), and the most important data are described in this section. All bed levels outside of the waterway were obtained from a digital elevation model with ninth arc-second (~3 m) resolution (CIRES 2014), merged with a 3 arc-second (~90 m) resolution digital elevation model from NOAA NCEI (2021) to extend to the north-eastern model

boundary, then reduced to 24 m resolution. In addition to the regional bathymetry map, a local, high resolution sonar bathymetric survey was conducted in cross sections approximately every 300 m throughout the waterway. These data were combined with existing bathymetric data gathered during pre-dredging and post-dredging surveys conducted in 2019 and 2020 (Atkins Engineering 2020).

The model was forced by 3 open boundaries from the surrounding water bodies: Myakka River at North Port Charlotte, Peace River at Harbor Heights, and Charlotte Harbor. Both the Myakka River and Peace River flow boundaries were imposed as a water level time series at 15-min intervals (USGS 2021a; USGS 2021b), while the Charlotte Harbor tidal boundary was forced by water levels at 1-h intervals. The rivers were forced as water level boundaries because of the availability of high-resolution (15-min) water level time-series records in this data scarce region. Model simulations using calculated discharge values from cumulative upstream discharge data at the river boundaries resulted in very similar velocity values (R^2 greater than 0.96) when compared with water level boundaries at the Ohara connection in the Manchester Waterway over a 1-month period. This period (July 2021) included the passage of Hurricane Elsa. Moreover, velocity comparisons between baseline and reconnection scenarios were indistinguishable for both boundary types.

Myakka River and Peace River temperature boundaries were forced by time-series data gathered from the Coastal & Heartland National Estuary Partnership Water Atlas (CHNEP 2021). River salinity boundaries were set to a constant value of 0 ppt to represent an inflow of freshwater. Charlotte Harbor water level, salinity, and temperature boundary data were gathered from the Hybrid Coordinate Ocean Model (HYCOM) + NCODA Gulf of Mexico 1/25° analysis hindcast dataset (Naval Research Laboratory 2022). Wind speed and direction data sourced from the closest weather station located at Fort Myers, Florida, approximately 40 km southeast of the waterway, was incorporated into the model as a constant time series at 1-h intervals (NOAA 2021a).

3.2 Model Calibration and Validation

Model performance was evaluated by comparing model simulated water levels to observed water surface elevations at 4 sites in the waterway over the period April 1, 2021–April 1, 2022. A record of surface water elevations was collected at Knox, Como, Gulfspray, and Site C (see locations in Fig. 1) for the period March 29, 2021–July 1, 2022. The model was calibrated by varying the Manning roughness coefficient because sensitivity analyses and existing literature (Bastidas et al. 2016) showed that water levels are significantly more sensitive to changes in the bed roughness compared to the physical parameters of horizontal eddy viscosity and horizontal eddy diffusivity (Table S1 in the Supplementary Material). Model performance was evaluated using four statistical measures: root mean square error (RMSE), Nash-Sutcliffe efficiency (NSE), percent bias (PBIAS), and R^2 coefficient of determination.

3.3 Modeling Scenarios

Four different weather conditions were considered for this study to evaluate how the reconnection alternative may respond under future and/or extreme weather conditions compared to the present land configuration. The

different scenarios were evaluated by changing the water level and wind surface boundaries that characterize the 4 environmental conditions of interest:

> **Condition 1: 2021–2022 Weather**
> Recorded environmental conditions for April 1, 2021–April 1, 2022
>
> **Condition 2: 2040 Sea Level Rise (SLR)**
> Increased boundary water levels to represent the 2040 SLR projections
>
> **Condition 3: Extreme Weather (EW)**
> Recorded water levels and wind speeds during Hurricane Eta
>
> **Condition 4: Cumulative Impact of an Extreme Weather Event + Sea Level Rise (EW+SLR)**
> Combination of Conditions 1 and 2

The proposed reconnection was simulated separately and compared to a baseline evaluation (BL) representing the present-day terrain in the Manchester Waterway. Thus, for each weather condition there were 2 different simulations representing the baseline and hydraulic reconnection, culminating in a total of 8 model simulations. The model setup was identical for the hydraulic reconnection, with the exception of changes to the bed levels to represent the depth, length, and width of constructed channels at the locations of the 3 proposed connections between Manchester Waterway and the harbor. The proposed connection between Tippecanoe Bay and the O'Hara Waterway through Muddy Cove is approximately 2,000 m, the second connection between Tippecanoe Bay and the intersection of the Flamingo and O'Hara waterways through Muddy Cove is approximately 2,530 m, and the connection between Myakka River and the intersection of the Como and O'Hara waterways has a channel length of approximately 2,180 m (see locations in Fig. 1). The bathymetry was adjusted for each navigational channel to best represent 12-meter-wide channels box cut to -1.6 m, based on the North American Vertical Datum of 1988 (NAVD 88).

The 2021–2022 weather condition was setup with hydrological and HYCOM boundary data spanning one year characterized by 124 cm of precipitation in Charlotte County, representing both dry and wet season conditions for the area. This year was representative of typical weather conditions for the area, for Charlotte County receives an annual average of 130 cm of rainfall, based on a historical record of 127 years (NOAA NCEI 2023).

To investigate the extent to which changing the waterway structure may have the potential to impact water movement in the waterway, extreme conditions were also tested. According to the NOAA Office for Coastal Management (2021b), there is an intermediate likelihood that the sea level will rise by 0.31 m by the year 2040 in the Fort Myers, Florida, region. Thus, the harbor and river boundary water levels were increased by 0.31 m to evaluate the baseline and connection alternative for the 2040 SLR projection condition (SLR).

To test the system during an extreme weather event (EW), reconnection alternative water levels were compared to the existing land configuration under the weather conditions of Hurricane Eta, which passed through the Gulf of Mexico near Charlotte Harbor as a Tropical Storm on November 12, 2020 (Pasch et al. 2021). This storm event was characterized by heavy rainfall (4.7 cm in 24 h, a rainfall event with approximately 7-month return interval; SWFWMD 2023), and recorded wind speeds at the nearest weather station in Fort Myers reached 15 kts (28 km/h), which exceed the 90th percentile mean hourly wind speeds of 13 kts for this region in November (Weather Spark 2023). Although this observed speed is below the tropical storm threshold, Eta was the most extreme weather event encountered in the region in recent times for which we can verify the model's input data. The storm surge resulting from these conditions is simulated in the model by imposing the hourly measured wind speeds at Fort Myers and forcing the 3 boundaries with water levels for the dates November 5–19, 2020.

The last scenario considered was a combination of a storm event and sea level rise conditions (EW+SLR). To simulate these future environmental conditions, the same model setup was used as the EW condition, with the harbor and river boundaries increased by 0.31 m as described in the SLR condition, and the model was simulated once again for the dates November 5–19, 2020.

The resulting surface water elevations and velocities under baseline and proposed reconnection conditions were compared for each scenario. Visual inspection of time-series and model-generated maps indicated changes to flow trends, as well as comparison of maximum, minimum, range, and average values over the simulation periods. Three primary locations within the waterway are the focus of analysis: Flamingo, Ohara, and Como, which are located at the waterway entrance to each of the proposed constructed channels through the barrier peninsula, in addition to Site C, which is situated southeast from the connections and is used to demonstrate the extent of influence to which the proposed connections would change water levels and velocities (see Fig. 1).

4. Results

4.1 Model Calibration and Validation

The calibrated RMSE at four sites in the waterway was 0.10–0.14 m and for validation was 0.11–0.15 m. This accuracy is satisfactory and consistent with other coastal modeling studies that calibrated models to RMSE of 0.08–0.28 m (Green et al. 2018; Stark et al. 2016; Yang et al. 2010; Smolders et al. 2015). Results of model calibration (April 1, 2021–September 30, 2021) determined that a spatially uniform Manning roughness coefficient of 0.006 was required to produce the tidal amplitudes observed in the waterway. The model has a tendency to underestimate water levels during months of heavy rainfall, and overestimate water levels during dry seasons as indicated by the PBIAS values in Table 1, reflecting on how the simulated waterway is strongly responsive to tidal influence and less sensitive to seasonal river fluctuations. The simulated tidal range in the waterway is also less than the observed range (0.11 m, 0.08 m, 0.1 m, and 0.27 m less at Knox, Como, Site C,

and Gulfspray, respectively, during validation period), with the site located in a canal furthest from the harbor (Gulfspray) exhibiting the greatest difference from measured surface water elevations. A comparison of model simulated and measured water surface elevations during the weeks of July 1–14, 2021, is provided in Fig. 4, showing that the model captures peak water levels during storm events. During that time, Hurricane Elsa passed through the Gulf of Mexico approximately 110 km off the coast of Florida as a Category 1 Hurricane, bringing with it a total of 28 cm of rainfall to Port Charlotte and maximum sustained winds of 32 kts with 38-kt gusts in Charlotte Harbor (NOAA 2022).

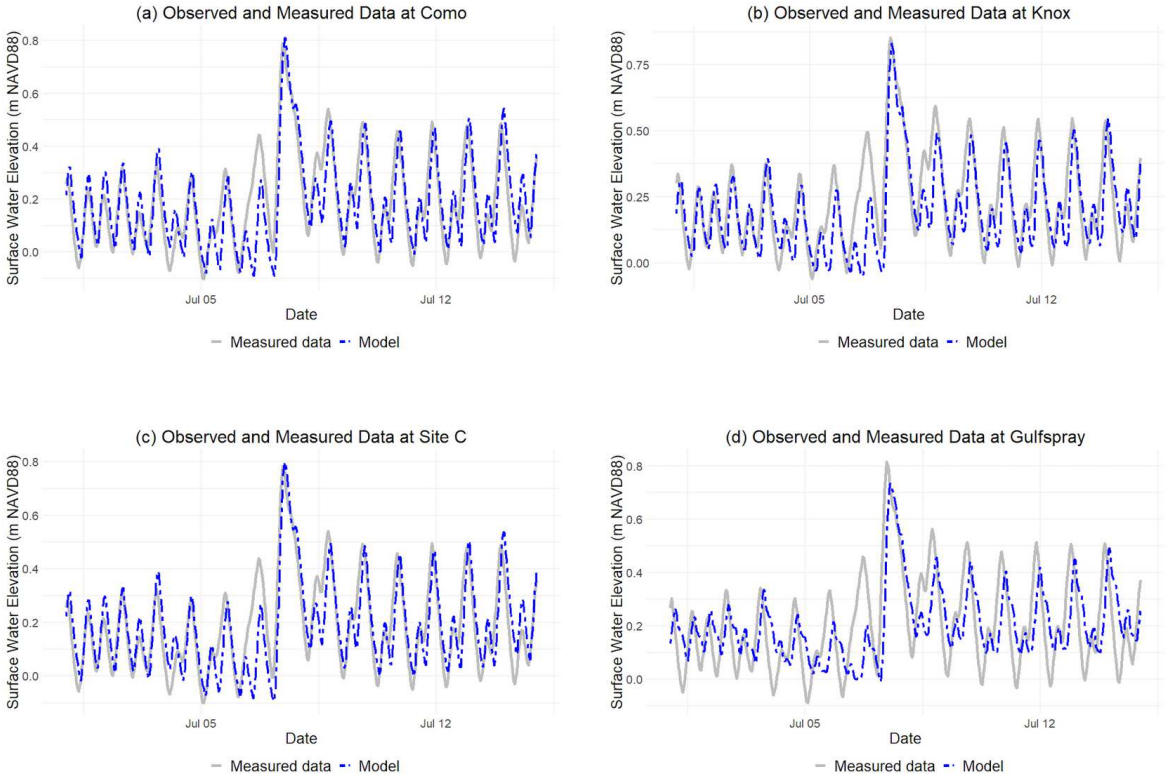

Fig. 4. Time series of measured (grey solid line) and simulated (blue dashed line) surface water elevations in July 2021. See Fig. 1 for locations.

Table 1 Model performance for water levels (m)

	Calibration (Apr. 1, 2021 – Sep. 30, 2021)				Validation (Oct. 1, 2021 – Apr. 1, 2022)			
Site	**RMSE**	**NS**	**PBIAS**	**R^2**	**RMSE**	**NS**	**PBIAS**	**R^2**
Knox	0.12	0.51	-17.03	0.57	0.12	0.60	-11.93	0.62

Como	0.10	0.64	-2.53	0.65	0.11	0.69	1.53	0.70
Site C	0.10	0.68	-1.70	0.67	0.11	0.70	12.61	0.71
Gulfspray	0.14	0.49	-0.60	0.27	0.15	0.42	7.87	0.43

4.2 Condition 1: 2021–2022 Weather

For the baseline evaluation of existing conditions from April 2021–April 2022, surface water elevations fluctuated uniformly with the tides at Flamingo, Ohara, Como, and Site C. The overall tidal range was the greatest at Como with 1.16 m, and smallest at Ohara with 1.12 m during the simulation period. The average water elevation was 0.2 m (NAVD 88).

Model outputs for the harbor side of the barrier peninsula exhibited greater range in tidal fluctuations, with high and low peaks exceeding those within the waterway. The tidal range over the evaluation period in Tippecanoe Bay was 1.7 m. Locations within the waterway tended to reach high tide and low tide approximately 2 h after Tippecanoe Bay, demonstrating how the existing narrow connections to the harbor at the east of the waterway cause a delay in tidal water movement.

Velocities in the waterway reached maximum speeds just before high and low tide, with greater simulated velocities during flood tide as compared to ebb tide (Fig. 5). Site C exhibited the greatest average velocities (0.27 m/s), followed by Como (0.17 m/s), Flamingo (0.14 m/s), and lastly Ohara (0.09 m/s). Site C typically reached maximum velocities of approximately 0.5 m/s, while Flamingo, Ohara, and Como reached maximum values of about 0.3 m/s during flood currents. During Hurricane Elsa (July 2021), Site C reached a maximum of 0.84 m/s while Flamingo, Ohara, and Como peaked at velocities of 0.41 m/s, 0.40 m/s, and 0.27 m/s, respectively (Fig. 5).

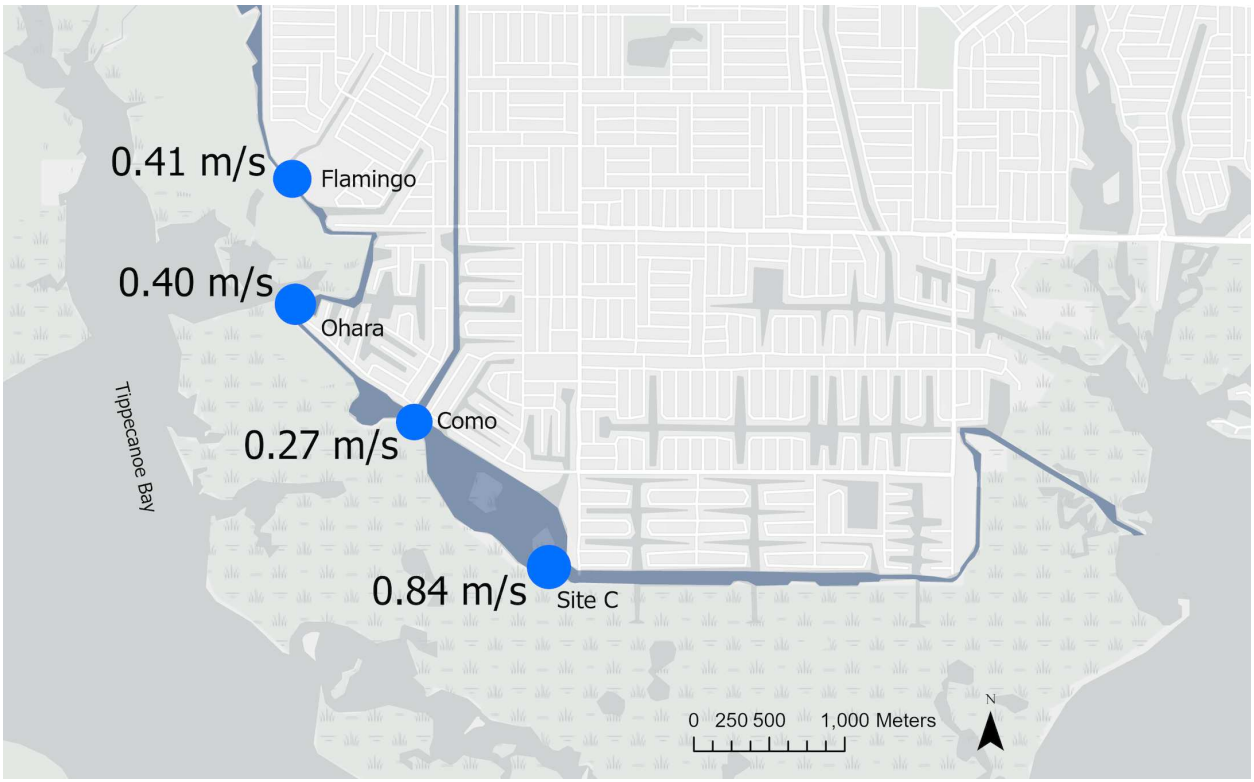

Fig. 5. Maximum velocity magnitudes simulated during Hurricane Elsa (July 6–8, 2021) for Condition 1: 2021–2022 Weather. (Map created using ArcGIS 2.7.0 software by Esri. ArcGIS is the intellectual property of Esri and is used herein under license.)

Surface water elevations for the proposed hydraulic reconnection were simulated by the model for the same time period as the baseline condition. Model results show that tidal amplitudes are greater under the reconnection scenario throughout the waterway (Fig. 6), with influence on water elevations decreasing further from existing connections. The simulated reconnection scenario resulted in a 10% to 17% increase in tidal range at the analysis sites Ohara, Flamingo, and Como, and a 15% to 18% decrease in average water levels due to an asymmetric response to tidal fluctuations. Water levels would be lower at low tide under the proposed connections, with the Ohara connection exhibiting the greatest change in minimum water level over the simulation period of 16 cm (-80%) (Table 2). While these differences are notable, they are not expected to pose a major navigational challenge because at the lowest levels, at least approximately 1 m of water depth is maintained in the middle of the channels.

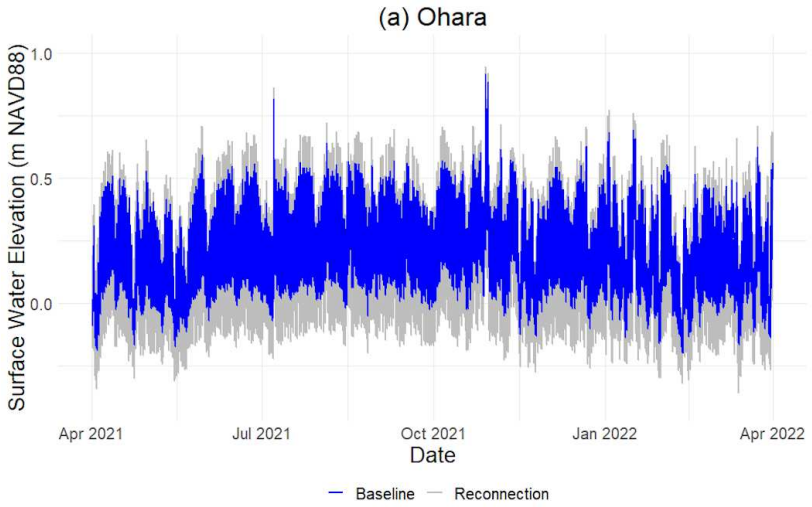
(a) Ohara
Surface Water Elevation (m NAVD88)
1.0
0.5
0.0
Apr 2021
Jul 2021
Oct 2021
Jan 2022
Apr 2022
Date
Baseline
Reconnection

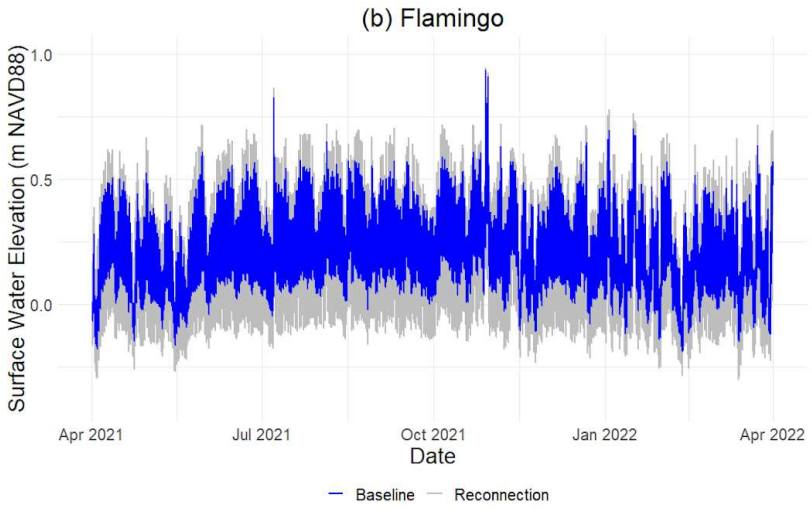
(b) Flamingo
Surface Water Elevation (m NAVD88)
1.0
0.5
0.0
Apr 2021
Jul 2021
Oct 2021
Jan 2022
Apr 2022
Date
Baseline
Reconnection

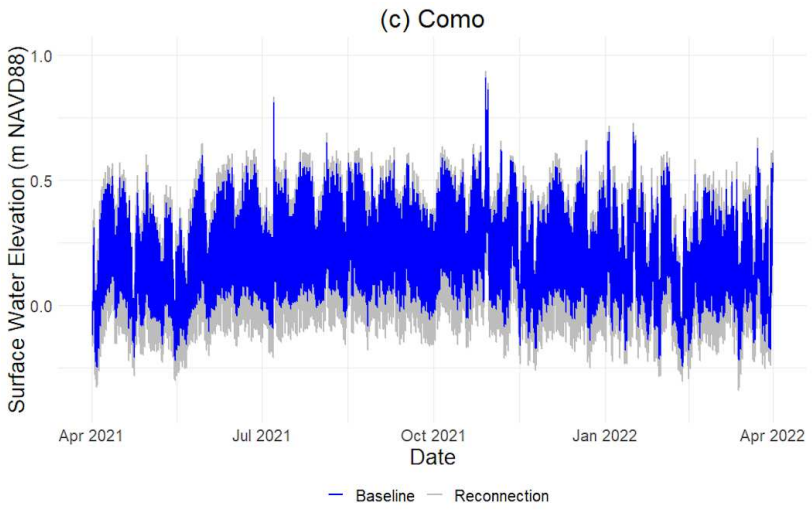
(c) Como
Surface Water Elevation (m NAVD88)
1.0
0.5
0.0
Apr 2021
Jul 2021
Oct 2021
Jan 2022
Apr 2022
Date
Baseline
Reconnection

Fig. 6. Surface water elevations for baseline and reconnection simulations from April 2021–April 2022 (Condition 1) at a) Ohara, b) Flamingo, and c) Como.

Table 2 Summary of surface water elevations and comparison between baseline and hydraulic reconnection for 2021–2022 weather conditions (m). See Fig. 1 for locations.

Site	Statistic	Baseline	Reconnection	% Change from BL
Ohara	max	0.92	0.95	2.97
	min	-0.20	-0.36	-79.72
	range	1.12	1.30	16.69
	avg	0.20	0.16	-17.75
Flamingo	max	0.93	0.95	1.21
	min	-0.19	-0.30	-60.05
	range	1.12	1.25	11.06
	avg	0.20	0.17	-16.56
Como	max	0.91	0.93	2.75
	min	-0.25	-0.34	-37.48
	range	1.16	1.27	10.14
	avg	0.19	0.16	-14.91

In addition to an increase in the tidal range, Fig. 7 demonstrates a shift in the tidal phase induced by the proposed connections. The model simulations show that with the proposed connections, water elevations would peak earlier than the baseline at high tide and low tide, reducing the lag time between tidal fluctuations in the harbor and the waterway. For instance, at Ohara a tidal phase shift of up to 1 h 30 min was simulated under proposed conditions, while at Flamingo and Como, shifts of up to 60 min and 30 min are projected, respectively. The changes in tidal range and tidal phase shift can be attributed to a reduction in the length of the path that water would travel to reach locations further from the harbor in the waterway and correspondingly a reduction in the effects of frictional forces encountered. The largest phase shift is simulated at Ohara, which is located furthest from any substantial water connection to the harbor under present environmental conditions.

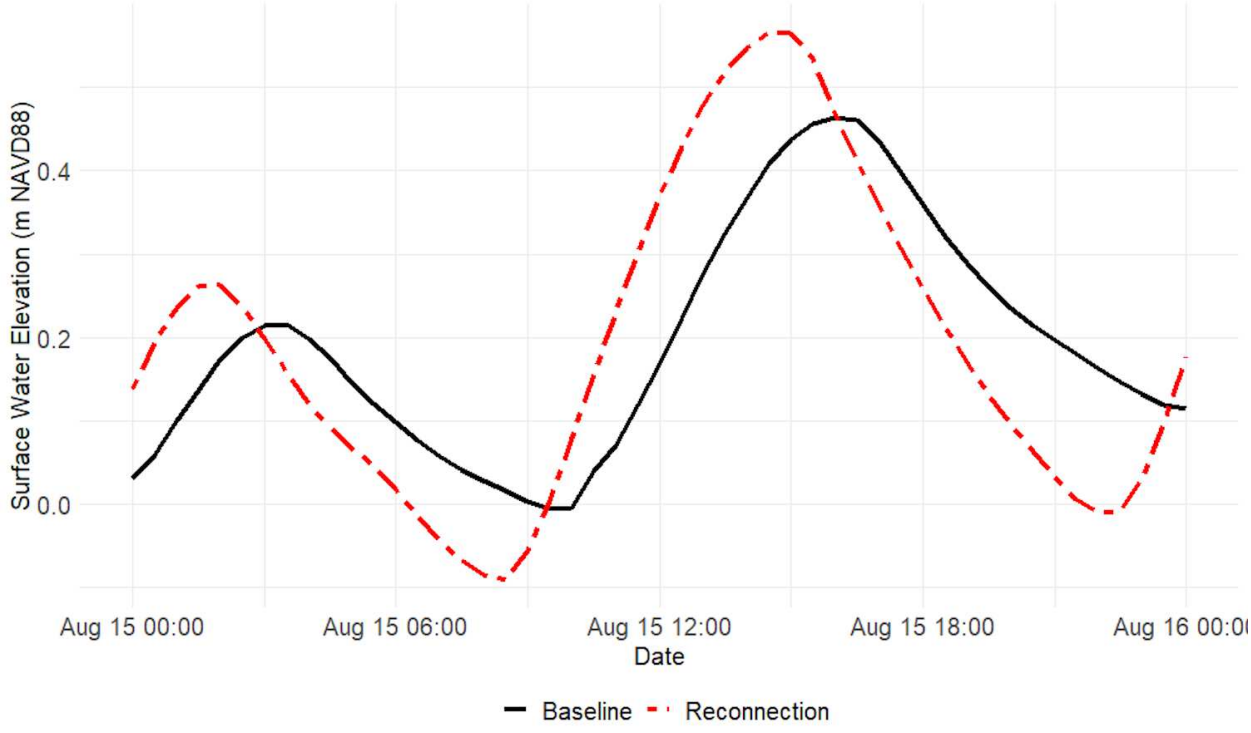

Fig. 7. Surface water elevations for baseline and reconnection simulations over a 24-h period at Ohara (Condition 1: 2021–2022 Weather). Plots for Flamingo and Como are provided in the Supplementary Material (Fig. S1).

Velocities are expected to change locally at the connection entrances in the waterway compared to the baseline. While in the baseline condition Ohara exhibited the lowest average velocity (0.09 m/s) compared to Flamingo (0.14 m/s) and Como (0.17 m/s), simulated velocities at this location would become the highest (0.18 m/s) under proposed conditions, showing considerable change to the system. Hydraulic reconnection increased the maximum velocity by 0.30 m/s (+57%) and average by 0.08 m/s (+87%) at Ohara, reduced the maximum by 0.03 m/s (-7%) and increased the average by 0.003 m/s (+2%) at Flamingo, and reduced the maximum by 0.11 m/s (-19%) and average by 0.05 m/s (-26%) at Como.

4.3 Condition 2: 2040 Sea Level Rise

The SLR condition was simulated for the same time period as the 2021–2022 weather condition, spanning one year. As expected, a simulated increase in water levels of 0.31 m for all boundary flows caused a corresponding increase in average water levels of 0.29 m–0.31 m at all locations in the waterway for the baseline and hydraulic reconnection relative to the 2021–2022 weather condition. Along with an increase in water elevations, the tidal range increased at all analysis sites throughout the waterway. The overall range in water elevations for the simulation period increased by 0.22 m–0.32 m at each site.

Comparing the hydraulic reconnection to the baseline for the SLR condition, the percent change for maximum, range, and average water elevations are all less than for the 2021–2022 weather condition, demonstrating that at higher sea levels the relative effect of connectivity between the harbor and waterway on water elevations is reduced (Table S3 in the Supplementary Material). Therefore, it is expected that as the mean height of sea level rises, differences in flow caused by changes to connectivity between the waterway and harbor will be less pronounced.

Similar water level elevations are predicted during high tide for the hydraulic reconnection and baseline scenarios due to flooding of the vegetated barrier peninsula under both conditions at these extreme water levels (Fig. 8). During lower high tides there is still a phase shift, but to a lesser degree than during the 2021–2022 weather condition, indicating some inundation of the barrier peninsula as well. At Flamingo, for instance, in the historical scenario where there was a tidal phase shift of approximately 1.5 h between reconnection and the baseline, in the SLR scenario the shift was reduced to 60 min.

The difference in water velocity between the hydraulic reconnection and baseline vary by location in the waterway for the year-long simulation period. The model results predict that reconnection would increase the maximum velocity by 0.315 m/s (+66%) and the mean velocity by 0.101 m/s (+116%) at Ohara, but would reduce the maximum by 0.007 m/s (-1.7%) and mean by 0.003 m/s (-1.6%) at Flamingo, and reduce the maximum by 0.103 m/s (-14%) and increase the average by 0.002 m/s (+0.9%) at Como.

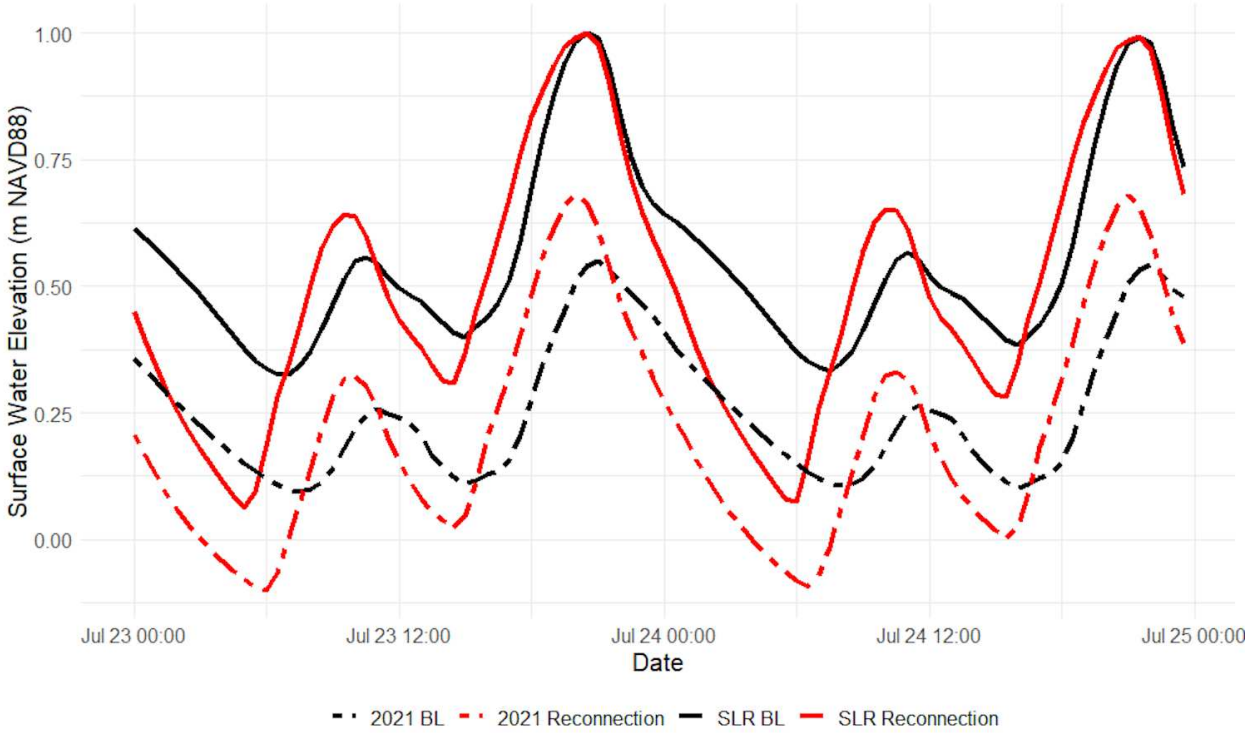

Fig. 8. Surface water elevations for 2021–2022 weather and SLR (Condition 2: 2040 Sea Level Rise) at Flamingo. Plots for Ohara and Como are provided in the Supplementary Material (Fig. S2).

4.4 Condition 3: Extreme Weather

Two-week simulations, which span 1 week before and after Hurricane Eta, show an increase in tidal amplitudes due to hydraulic reconnection compared to the baseline as observed in the previous weather conditions. Water elevations and tidal phases were nearly identical, however, for the duration of the storm event (0000 to 1300 on November 12, 2020, Fig. 9). In all simulations and at all locations of interest in the waterway, the water levels peaked on November 12, 2020, from 0530 to 0545, and the difference in maximum water surface elevation between the baseline and proposed reconnection did not exceed 0.3 cm (Table S4 in the Supplementary Material). While surface water elevations converge during the storm event, time series plots show that following the peak of the storm event, water levels drop to lower elevations and at a faster rate for the reconnection scenarios than for baseline condition.

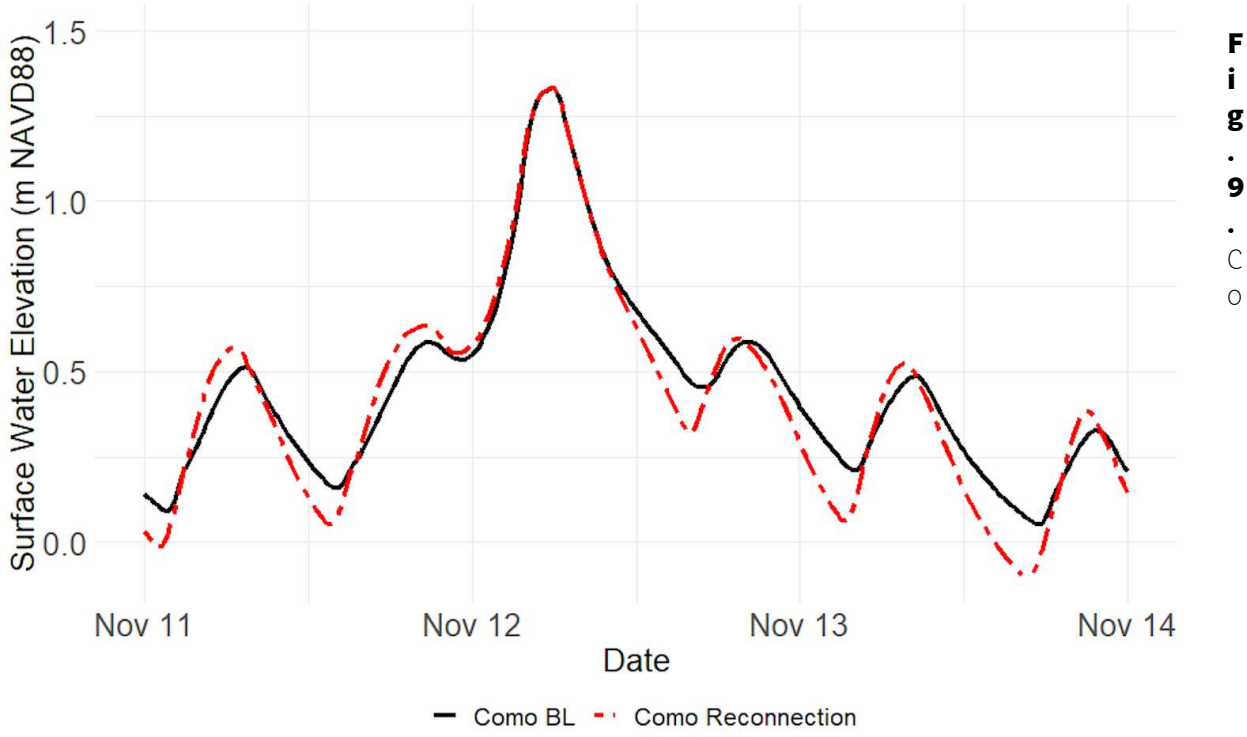

Fig. 9. Comparison of surface water elevations at Como during Hurricane Eta (Condition 3: Extreme Weather). Plots for Ohara and Flamingo are provided in the Supplementary Material (Fig. S3).

The proposed hydraulic reconnection simulation demonstrated local influence on velocities in the waterway during the storm event. The geographic extent of influence on velocity magnitudes in the waterway for each connection option is depicted in Fig. 10, which shows the mean difference in velocity between the baseline and

reconnection at 0200 on November 12, 2020. During the storm for the baseline condition, maximum water velocities at Flamingo, Ohara, Como, and Site C reached magnitudes of 0.27 m/s, 0.26 m/s, 0.71 m/s, and 1.16 m/s, respectively. Maximum velocity magnitudes at Flamingo, Como and Site C decreased by 0.04 m/s (-14%), 0.08 m/s (-11%), and 0.12 m/s (-10%), respectively as a result of reconnection in comparison to the baseline during the storm event, while they increased at Ohara by 0.07 m/s (+27%). Average velocities differed by 0.02 m/s to 0.08 m/s.

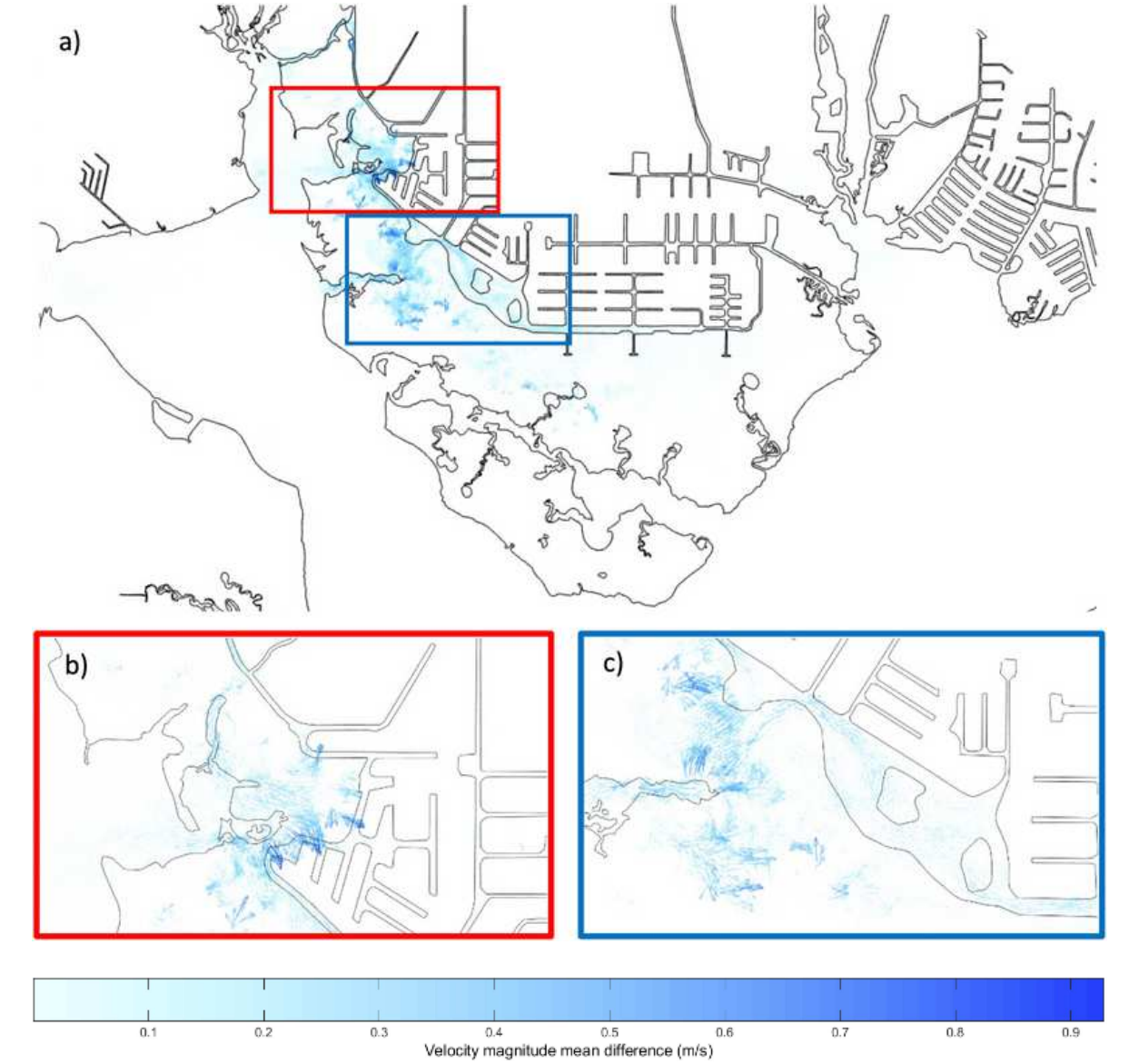

Fig. 10. Difference in mean velocity between baseline and reconnection at 0200 during November 12, 2020, storm event (Hurricane Eta). a) Manchester Waterway and surrounding waters, b) Close-up

of Ohara and Flamingo connections, c) Close-up of Como connection. (Maps created using Deltares post-processing tool, Delft3D-QUICKPLOT.)

4.5 Condition 4: Extreme Weather + Sea Level Rise

The final weather condition evaluated, Extreme Weather + Sea Level Rise (EW+SLR), predicts behavior of the system under future extreme conditions, a demonstration that is critical to include in analysis for coastal planning and restoration. Similar to results for the EW condition, surface water elevations as a result of reconnection show little deviation from the baseline, such that timing and maximum elevations of water levels are synchronized during the storm event. The maximum elevation for all locations evaluated differed by no more than 0.1 cm, however the minimum elevations at all sites were lower in the hydraulic reconnection simulation than the baseline for all sites (Table 3). During the storm event, maximum velocities decreased (0.01 m/s–0.04 m/s) while average velocities increased (0.01 m/s–0.03 m/s) at Flamingo, Ohara, and Como, compared to the baseline.

Table 3 Summary of surface water elevations (m) during the hours of 0000 to 1300 of the November 12, 2020, storm event in combination with sea level rise (Condition 4: EW+SLR)

Site	Statistic	Baseline	Reconnection	% Change from BL
Ohara	max	1.69	1.69	0.07
	min	0.69	0.57	-18.44
	range	1.00	1.13	12.93
	avg	1.21	1.20	-1.33
Flamingo	max	1.71	1.71	0.00
	min	0.68	0.56	-17.86
	range	1.03	1.15	11.83
	avg	1.22	1.20	-1.65

Como	max	1.64	1.64	0.01
	min	0.70	0.66	-5.19
	range	0.94	0.97	3.90
	avg	1.20	1.19	-0.33

5. Discussion

Coastal engineering activities have disrupted estuarine ecosystems in many parts of the world and in some cases have created unanticipated challenges for coastal communities (Jones et al. 2012; Rangel-Buitrago et al. 2018; Silver et al. 2019). The construction of housing developments in the Manchester Waterway has created a fundamentally different system, thus optimal flow conditions for this system may be assessed by predicted risk to the local community and impact to ecosystem health based on environmental indicators, rather than a return to historic conditions. Improving hydraulic connectivity between Manchester Waterway and Charlotte Harbor has the potential to restore some environmental functions by creating channels that emulate tidal creeks, thereby increasing exchange of water between the harbor and the open ocean through the barrier peninsula. Changes to hydraulic connectivity have been shown to impact estuarine ecology in some regions, such as the change in dominant plant species and subsequent increase of bird population and species observed following reconnection of river flow to the Yellow River Delta, China (Jiang et al. 2021). In Great South Bay, New York, for instance, shellfish production increased following the opening of an inlet which increased flushing (Gobler et al. 2019). Along the west coast of Florida, it was suggested that estuarine flow velocities and flushing rates be altered to reduce destructive *K. brevis* blooms, also known as “red tide” (Yentsch et al. 2008). The proposed hydraulic reconnections would certainly be the first step in a potential ecological restoration plan for the region, though such a plan has not yet been created. Still, given limited historic hydrodynamic, water quality, and biological data for this system, restoration to “pristine” conditions would be challenging.

5.1 Surface Water Elevations

Because homes in the case study community are situated along the edge of the waterway, they are vulnerable to flooding and storm surge caused by elevated water levels. The concern expressed by community members about hydraulic reconnection is increased flooding owed to the additional tidal inlets through the protective barrier peninsula for storm surge to funnel through. Reconnection of the waterway to the open estuary is expected to increase maximum and average surface water elevation, therefore these indicators are of primary concern. Results of this study show that tidal amplitude and high tide surface water elevations under average flow conditions are expected to increase as a result of reconnection (Fig. 6), though not by a magnitude that would cause an increased risk of flooding, which would occur with the breach of residential seawalls (approximately 0.9 m NAVD88; NOAA 2021b), to the community during the regular tidal cycle. These

findings are consistent with the results of other studies that have associated increased channel depths with an increase in tidal amplitudes (Jay et al. 2011; Vellinga et al. 2014) and a decrease in the tidally averaged water levels in some estuarine systems, attributed to frictional effects (Ralston et al. 2019). Potentially impactful to local residents is the lowering of water levels at low tide under proposed conditions, which could pose a navigational challenge in the already shallow channels.

Table 4 Heat map of percent change in surface water elevations between the proposed hydraulic reconnection and baseline configurations for each weather condition and analysis site

	Historical				SLR				EW				EW + SLR			
Site	**max**	**avg**	**min**	**range**	**max**	**avg**	**min**	**range**	**max**	**avg**	**min**	**range**	**max**	**avg**	**min**	**range**
Ohara	3	-18	-80	17	0	-9	-318	15	0	-2	-28	19	0	-1	-18	13
Flamingo	1	-17	-60	11	0	-9	-409	13	0	-2	-33	22	0	-2	-18	12
Como	3	-15	-37	10	0	-6	-168	12	0	0	0	1	0	0	-5	4

Model evaluations show that storm surge is anticipated to reach the same maximum elevation under both baseline and reconnection conditions for storm events (Table 4), as shown in evaluations of Hurricane Eta and Hurricane Elsa. This shows that reconnection would cause minimal change to high water levels during flood events, although the simulated decrease in low tide following storm surge may provide additional relief to the system by reducing the duration of flooding events. The evaluation of a hydrodynamic model validated in the local Manchester Waterway presented here provides a high-resolution assessment of water flow in a residential waterway as compared to large scale models of Charlotte Harbor, which yield regional results of circulation (Chen 2020; Kim et al. 2010; Liu et al. 2020; Zheng and Weisberg 2004). The simulated increase in tidal range has ecological implications, for tidal amplitude heavily influences the distribution and characteristics of estuarine vegetation (McLusky and Elliott 2004). This is especially relevant in flat shorelines common to Florida, where a small increase in water level could have an exponential increase in inundation area. Some of the shoreline habitats that have historically always been inundated may experience regular dry periods during the tidal cycle, and habitats that are rarely inundated may experience regular flooding, potentially increasing the area available for mangrove establishment.

5.2 Velocities

Model results show that changes to velocity magnitudes are dependent on the location in the waterway due to variations in circulation patterns. Increased connectivity and water exchange with the harbor is expected to cause an increase in maximum and mean velocities at Ohara, which is furthest from any existing connection to the harbor but would be located at a waterway connection under the proposed connections. The changes are most pronounced under sea level rise conditions at Ohara, during which the mean velocities are predicted to double due to the proposed reconnections. Conversely, a decrease in velocity magnitudes at Flamingo and

Como is expected under typical weather conditions (Table 5), though changes are less than those predicted at Ohara. Because erosion rates are a function of water velocity, higher velocity magnitudes pose the risk of increased erosion in the waterway, while lower velocities may cause increased sediment deposition (Earle 2019; Simms 2023; Wolanski et al. 1995). Changes to the current velocities occurring during flood and ebb currents have the potential to alter sediment transport processes and consequently, long-term estuarine morphodynamics (Stark et al. 2017). Investigation of sediment characteristics (particle size, density) in the waterway would be needed to estimate critical erosion velocities, particularly at Ohara, and to predict whether any resulting erosion rates and concentrations of suspended particulate matter exceed a given threshold (Widdows et al. 1998). Such processes should be considered in future research. Moreover, flow velocities have been shown to have an impact on marine intertidal community structure, such as the difference in barnacle density observed between areas of low-flow and high-flow sites in a Maine estuary (Leonard et al. 1998). Habitat distribution in the Manchester Waterway thus has the potential to be altered by changes to velocity patterns.

Table 5 Heat map of percent change in water velocities between the proposed hydraulic reconnection and baseline configurations for each weather condition and analysis site

	Historical				SLR				EW				EW + SLR			
Site	**max**	**avg**	**min**	**range**	**max**	**avg**	**min**	**range**	**max**	**avg**	**min**	**range**	**max**	**avg**	**min**	**range**
Ohara	57	87	0	57	66	116	0	66	27	73	213	22	-14	11	9	-16
Flamingo	-7	2	0	-7	-2	-2	0	-2	-14	18	161	-22	-2	33	693	-36
Como	-19	-26	0	-19	-14	1	0	-14	-11	25	472	-30	-4	2	20	-6

5.3 Sea Level Rise

There remain critical opportunities to design sustainable coastal restoration projects using hydrodynamic modeling to simulate system response under expected future environmental conditions. This study contributes to the body of literature investigating the impact of sea level rise on estuarine environments, by assessing the influence on water level and velocity trends of designed—but not yet constructed—local geomorphological modifications.

Model results of the Manchester Waterway show that the tidal range is expected to increase with rising sea levels, consistent with the findings of other studies that conclude that sea level rise in estuaries will result in a larger tidal prism (Khojasteh et al. 2021; Passeri et al. 2016). This response is amplified under the proposed reconnection scenarios that further increase the cross-sectional flow area available at the waterway entrances. Due to increased inundation of the barrier peninsula under 2040 SLR projections, surface water elevations at high tide would become more similar between baseline and the proposed reconnection channel configurations than under present day water elevations, while differences at low tide would be amplified. When considering

the combined effects of SLR and an extreme weather event, the predicted difference in maximum storm surge is negligible (<0.1 cm).

5.4 Future Research

This study demonstrates the application of a high-resolution, unstructured grid hydrodynamic model to evaluate 2D water movement in an estuarine system. The modeling approach used in this study is based on necessary simplifying assumptions that make numerical evaluations computationally possible. Impacts to coastal water circulation resulting from the hydraulic reconnections can, in turn, rearrange estuary structure as the system reaches a new equilibrium state (Elliott et al. 2016). Therefore, modeling of sediment transport and erosion should also be conducted to account for land morphological change over time. This would assess the longevity of restoration projects and inform what maintenance efforts may be required to sustain the new system, such as regular dredging or sediment stabilization. Because changes in tidal amplitude were observed in the model results, additional analysis should be conducted to assess the changes to tidal asymmetry, and, in turn, investigate how sediment transport would be affected (Stark et al. 2017).

Furthermore, altering the barrier island geomorphology has the potential to impact the coastal ecosystem in many ways that have not been considered here, some of which are complex and may result from a series of interactions. Additional analysis is required to predict the effect of such combined interactions. Ecohydrological modeling, for instance, could be conducted to incorporate the influences of dynamic ecological components and, in turn, assess the impacts to water quality, wildlife, and vegetation. Moreover, evaluation of salinity and temperature would serve as an initial indicator of changes to habitat conditions and the life that may be supported. The results of this study, for instance, could be combined with mapping of sediment characteristics and sensitive habitats to identify species that may benefit or be harmed by changes to connectivity and the tidal regime.

6. Conclusion

The 8 scenarios evaluated in this study (2 coastal configurations x 4 weather conditions) improve the understanding of this relatively unstudied, complex estuarine system, and the potential outcomes of hydraulic reconnections in similar coastal systems. Resulting water levels and velocities from model simulations predict future system behavior in the event that proposed reconnection plans are implemented or if the present spatial configuration is maintained. The model evaluations conducted in this study simplify the complex environmental characteristics that influence water movement and allow for the prediction of general flow patterns in the waterway. Following is a synthesis of the major findings: (1) Increased connectivity would increase tidal amplitudes, increase maximum water levels, decrease minimum water levels, decrease average water levels, and induce a tidal phase shift during average conditions; (2) During extreme weather events, maximum surface water elevations would be nearly equal for the hydraulic reconnection and baseline land configurations, though the reconnection would allow water levels to return to lower levels than the baseline; (3) Under 2040 sea level rise conditions, the difference in water elevations between the reconnection and

baseline configuration would be reduced; (4) Mean velocity magnitudes would increase in some parts of the waterway but decrease in others as a result of the hydraulic reconnection.

The value of hydrodynamic modeling prior to making transformative changes to the environment should not be underutilized, for it is a powerful tool that has the potential to deter the implementation of projects which may result in adverse outcomes. As advanced hydrodynamic modeling techniques improve, the ability to predict the outcomes of coastal ecological engineering activities is enhanced. While the hydrodynamics of coastal regions influenced by large-scale engineering projects have been evaluated in previous studies, the research presented in this paper exemplifies how modeling can be used as a tool at the local scale to evaluate site-specific flow conditions, and the effects of hydraulic reconnection and subsequent ecological restoration. This methodological approach should be used to support other small coastal communities in their efforts to sustain and restore environmental conditions.

Supplementary Material

The online version of this article contains a link to supplementary material that includes: **Table S1** Sensitivity Analysis; **Table S2** Model Database; **Table S3** Summary of surface water elevations (m) and comparison between baseline and reconnection (Condition 2: Sea Level Rise); **Table S4** Summary of surface water elevations (m) during the hours of 0000–1300 of the November 12, 2020, storm event (Condition 3: Extreme Weather); **Fig. S1** Surface water elevations for baseline and reconnection simulations over a 24-h period at a) Ohara, b) Flamingo, and c) Como (Condition 1: 2021–2022 Weather); **Fig. S2** Surface water elevations for 2021–2022 weather and SLR at a) Ohara, b) Flamingo, and c) Como (Condition 2: 2040 Sea Level Rise); **Fig. S3** Comparison of surface water elevations at a) Ohara, b) Flamingo, and c) Como during Hurricane Eta (Condition 3: Extreme Weather).

pdf JEED_Kramer_Arias_Supplementary_Material_060523.pdf 580 KB

Acknowledgements

This material is based on work supported by the National Science Foundation Collaborative Research Traineeship (NRT) Award No. 1735320. It was also supported financially by Charlotte County, Florida, and a Gulf Research Program Early Career Fellowship from the National Academy of Sciences. Special thanks to the Manchester Waterway Civic Association and community members for their continuous support during this study. Additional thanks to Dr. Thanh Dang and Dr. Ping Wang for their feedback and expertise. Any opinions, findings, and conclusions or recommendations expressed in this material are those of the authors and do not necessarily reflect the views of the funding organizations.

Author Contributions Statement

Conceptualization: MEA, MK; methodology: MEA, MK; data analysis: MK; writing original draft: MK; reviewing/editing original draft: MEA; investigation: MK; resources: MEA; data curation: MK; supervision: MEA; project administration: MEA; funding acquisition: MEA. All authors have read and agreed to the published version of the manuscript.

Conflict of Interest Statement

The authors have no conflict of interest to report.

Data Availability Statement

Most data used in this study are described in detail in the Methods section and in the Supplementary Materials (Table S2, specifically). Any additional data can be provided upon reasonable request.

Related Publication Statement

This study is based on the thesis work completed by Megan Kramer in partial fulfillment of the requirements for the degree of Master of Science in Environmental Engineering at the University of South Florida.

ORCID iDs

Megan Kramer https://orcid.org/0000-0001-6467-1960
Mauricio E. Arias https://orcid.org/0000-0002-8805-6353

References

Aretxabaleta AL, Butman B, Ganju NK. 2014. Water level response in back-barrier bays unchanged following Hurricane Sandy. Geophysical Research Letters. 41(9):3163–3171. https://doi.org/10.1002/2014GL059957.

Atkins Engineering. 2020. Manchester Waterway bathymetry pre- and post-dredging [unpublished dataset]. Atkins Engineers, Inc.

Bastidas LA, Knighton J, Kline SW. 2016. Parameter sensitivity and uncertainty analysis for a storm surge and wave model. Natural Hazards and Earth System Sciences. 16(10):2195–2210. https://doi.org/10.5194/nhess-16-2195-2016.

Brown S, Nicholls RJ, Woodroffe CD, Hanson S, Hinkel J, Kebede AS, Neumann B, Vafeidis AT. 2013. Sea-level rise impacts and responses: a global perspective. In: Finkl CW, editor. Coastal hazards. Dordrecht: Springer Netherlands. (Coastal Research Library). p. 117–149. [accessed 2022 Aug 25]. https://doi.org/10.1007/978-94-007-5234-4_5.

Chen X. 2020. Hydrodynamic simulations of Charlotte Harbor and its major tributaries in Florida using a dynamically coupled 3D–2DV model. Estuarine, Coastal and Shelf Science. 246. https://doi.org/10.1016/j.ecss.2020.107026.

[CHNEP] Coastal and Heartland National Estuary Partnership. 2021. Charlotte Harbor Estuaries volunteer water quality monitoring network [database; accessed 2022 Apr 10]. https://chnep.wateratlas.usf.edu/chevwqmn/.

[CIRES] Cooperative Institute for Research in Environmental Sciences. 2014. Continuously updated digital elevation model (CUDE–) – ninth arc-second resolution bathymetric-topographic tiles [dataset]. NOAA National Centers for Environmental Information; [accessed 2021 Mar 8]. https://doi.org/10.25921/ds9v-ky35.

Deltares. 2021. Delft3D-FLOW User Manual. Deltares. https://content.oss.deltares.nl/delft3d4/Delft3D-FLOW_User_Manual.pdf.

Earle S. 2019. Physical geology. 2nd ed. BCcampus. Chapter 13.3, Stream erosion and deposition. [accessed 2023 Mar 13]. https://opentextbc.ca/physicalgeology2ed/chapter/13-3-stream-erosion-and-deposition/.

Elliott M, Mander L, Mazik K, Simenstad C, Valesini F, Whitfield A, Wolanski E. 2016. Ecoengineering with ecohydrology: Successes and failures in estuarine restoration. Estuarine, Coastal and Shelf Science. 176:12–35. https://doi.org/10.1016/j.ecss.2016.04.003.

[FDEP] Florida Department of Environmental Protection. 2005. Water quality assessment report–Charlotte Harbor. FDEP Division of Water Resource Management. [accessed 2022 Feb 1]. http://sarasota.wateratlas.usf.edu/upload/documents/Water%20Quality%20Assessment%20Report%20for%20the%20Charlotte%20Harbor%20Basin.pdf.

[FDEP] Florida Department of Environmental Protection. 2021. Gasparilla Sound–Charlotte Harbor Aquatic Preserve; [accessed 2021 Dec 30]. https://floridadep.gov/rcp/aquatic-preserve/locations/gasparilla-sound-charlotte-harbor-aquatic-preserve.

Florida State Parks. 2022. Charlotte Harbor Preserve State Park. [accessed 2022 Feb 1]. https://www.floridastateparks.org/parks-and-trails/charlotte-harbor-preserve-state-park.

George DA, Gelfenbaum G, Stevens AW. 2012. Modeling the hydrodynamic and morphologic response of an estuary restoration. Estuaries and Coasts. 35(6):1510–1529. https://doi.org/10.1007/s12237-012-9541-8.

Gobler CJ, Young CS, Goleski J, Stevens A, Thickman J, Wallace RB, Curran P, Koch F, Kang Y, Lusty MW, et al. 2019. Accidental ecosystem restoration? Assessing the estuary-wide impacts of a new ocean inlet created by Hurricane Sandy. Estuarine, Coastal and Shelf Science. 221:132–146. https://doi.org/10.1016/j.ecss.2019.02.040.

Google Earth Pro (7.3.6.9345). 2022 Apr 15. Charlotte Harbor, Florida Imagery, 26.9634657,-82.1674623. Image Landsat/Copernicus, Image © 2023 Maxar Technologies [accessed 2023 May 31]. https://earth.google.com/web/@26.9583937,-82.0670333,6622.97873637a,0d,35y,0h,0t,0r?utm_source=earth7&utm_campaign=vine&hl=en.

Green RH, Lowe RJ, Buckley ML. 2018. Hydrodynamics of a tidally forced coral reef atoll. Journal of Geophysical Research: Oceans. 123(10):7084–7101. https://doi.org/10.1029/2018JC013946.

Jay DA, Leffler K, Degens S. 2011. Long-term evolution of Columbia River tides. Journal of Waterway, Port, Coastal, and Ocean Engineering. 137(4):182–191. https://doi.org/10.1061/(ASCE)WW.1943-5460.0000082.

Jiang Y, Wang Y, Zhou D, Ke Y, Bai J, Li W, Yan J. 2021. The impact assessment of hydro-biological connectivity changes on the estuary wetland through the ecological restoration project in the Yellow River Delta, China. Science of The Total Environment. 758:143706. https://doi.org/10.1016/j.scitotenv.2020.143706.

Jones HP, Hole DG, Zavaleta ES. 2012. Harnessing nature to help people adapt to climate change. Nature Climate Change. 2(7):504–509. https://doi.org/10.1038/nclimate1463.

Khojasteh D, Glamore W, Heimhuber V, Felder S. 2021. Sea level rise impacts on estuarine dynamics: A review. Science of The Total Environment. 780:146470. https://doi.org/10.1016/j.scitotenv.2021.146470.

Kim T, Peter Sheng Y, Park K. 2010. Modeling water quality and hypoxia dynamics in Upper Charlotte Harbor, Florida, U.S.A. during 2000. Estuarine, Coastal and Shelf Science. 90(4):250–263. https://doi.org/10.1016/j.ecss.2010.09.006.

Kulp SA, Strauss BH. 2019. New elevation data triple estimates of global vulnerability to sea-level rise and coastal flooding. Nat Commun. 10(1):4844. https://doi.org/10.1038/s41467-019-12808-z.

Leonard GH, Levine JM, Schmidt PR, Bertness MD. 1998. Flow-driven variation in intertidal community structure in a Maine estuary. Ecology. 79(4):1395–1411. https://doi.org/10.1890/0012-9658(1998)079%5b1395:FDVIIC%5d2.0.CO;2.

Liu Y, Weisberg RH, Zheng L. 2020. Impacts of Hurricane Irma on the circulation and transport in Florida Bay and the Charlotte Harbor Estuary. Estuaries and Coasts. 43(5):1194–1216. https://doi.org/10.1007/s12237-019-00647-6.

Manchester Waterway Civic Association. 2021. History of Manchester Waterway. Manchester Waterway Civic Association. [accessed 2023 Mar 8]. https://manchesterwaterway.org/manchester-waterway.

McLusky DS, Elliott M. 2004. The estuarine ecosystem: ecology, threats and management. 3rd ed. New York (NY): Oxford University Press U.S.A. ISBN: 9780198525080.

Naval Research Laboratory. 2022. HYCOM + NCODA Gulf of Mexico [dataset; accessed 2022 Apr 10]. https://www.hycom.org/data/gomu0pt04/expt-90pt1m000.

[NOAA] National Oceanic and Atmospheric Association. 2021a. Fort Myers, FL meteorological observations [dataset; accessed 2022 Apr 12]. NOAA Tides and Currents. https://tidesandcurrents.noaa.gov/met.html?id=8725520.

[NOAA] National Oceanic and Atmospheric Association. 2021b. Sea level rise viewer. NOAA Office for Coastal Management. [accessed 2022 Feb 7]. https://coast.noaa.gov/slr/.

[NOAA] National Oceanic and Atmospheric Association. 2022. Tropical cyclone report: Hurricane Elsa. National Hurricane Center. [accessed 2023 Mar 10]. https://www.nhc.noaa.gov/data/tcr/AL052021_Elsa.pdf.

[NOAA NCEI] National Oceanic and Atmospheric Association National Centers for Environmental Information. 2021. Coastal relief model (3-second resolution) [dataset; accessed 2021 May 18]. National Oceanic and Atmospheric Association. https://www.ncei.noaa.gov/maps/grid-extract/.

[NOAA NCEI] National Oceanic and Atmospheric Association National Centers for Environmental Information. 2023. Climate at a glance county time series [dataset; accessed 2023 Mar 13]. https://www.ncei.noaa.gov/access/monitoring/climate-at-a-glance/county/time-series.

Pasch RJ, Reinhart BJ, Berg R, Roberts DP. 2021 National Hurricane Center tropical cyclone report: Hurricane Eta. National Hurricane Center. [accessed 2023 Mar 10]. https://www.nhc.noaa.gov/data/tcr/AL292020_Eta.pdf.

Passeri DL, Hagen SC, Plant NG, Bilskie MV, Medeiros SC, Alizad K. 2016. Tidal hydrodynamics under future sea level rise and coastal morphology in the Northern Gulf of Mexico. Earth's Future. 4(5):159–176. https://doi.org/10.1002/2015EF000332.

Prosser DJ, Jordan TE, Nagel JL, Seitz RD, Weller DE, Whigham DF. 2018. Impacts of coastal land use and shoreline armoring on estuarine ecosystems: an introduction to a special issue. Estuaries and Coasts. 41(1):2–18. https://doi.org/10.1007/s12237-017-0331-1.

Ralston DK, Talke S, Geyer WR, Al-Zubaidi HAM, Sommerfield CK. 2019. Bigger tides, less flooding: effects of dredging on barotropic dynamics in a highly modified estuary. Journal of Geophysical Research: Oceans. 124(1):196–211. https://doi.org/10.1029/2018JC014313.

Rangel-Buitrago N, Williams AT, Anfuso G. 2018. Hard protection structures as a principal coastal erosion management strategy along the Caribbean coast of Colombia. A chronicle of pitfalls. Ocean & Coastal Management. 156:58–75. https://doi.org/10.1016/j.ocecoaman.2017.04.006.

Silver JM, Arkema KK, Griffin RM, Lashley B, Lemay M, Maldonado S, Moultrie SH, Ruckelshaus M, Schill S, Thomas A, et al. 2019. Advancing coastal risk reduction science and implementation by accounting for climate, ecosystems, and people. Frontiers in Marine Science. 6. https://doi.org/10.3389/fmars.2019.00556.

Simms MJ. 2023. Tortoises, hares and the evolution of the Irish landscape. Geology Today. 39(1):13–17. https://doi.org/10.1111/gto.12416.

Smolders S, Plancke Y, Ides S, Meire P, Temmerman S. 2015. Role of intertidal wetlands for tidal and storm tide attenuation along a confined estuary: a model study. Natural Hazards and Earth System Sciences. 15(7):1659–1675. https://doi.org/10.5194/nhess-15-1659-2015.

Stark J, Plancke Y, Ides S, Meire P, Temmerman S. 2016. Coastal flood protection by a combined nature-based and engineering approach: modeling the effects of marsh geometry and surrounding dikes. Estuarine, Coastal and Shelf Science. 175:34–45. https://doi.org/10.1016/j.ecss.2016.03.027.

Stark J, Smolders S, Meire P, Temmerman S. 2017. Impact of intertidal area characteristics on estuarine tidal hydrodynamics: a modelling study for the Scheldt Estuary. Estuarine, Coastal and Shelf Science. 198:138–155. https://doi.org/10.1016/j.ecss.2017.09.004.

[SWFWMD] Southwest Florida Water Management District. 2023. Environmental data portal | water data viewer: ROMP TR 3-1 Suwannee [dataset]; [accessed 2023 Mar 10]. https://edp.swfwmd.state.fl.us/applications/login.html?publicuser=Guest#waterdata-external/stationoverview.

[USDA] United States Department of Agriculture. 1952. Aerial photographs of Charlotte County – Flight 1H (1942) [image; accessed 2023 May 24]. https://original-ufdc.uflib.ufl.edu/UF00071733/00004/8?search=charlotte+%3dcounty.

[USDA] United States Department of Agriculture. 1974. Aerial photographs of Charlotte County – Flight 274 (1974) [image; accessed 2023 May 24]. https://original-ufdc.uflib.ufl.edu/UF00071733/00028/8x?search=charlotte+%3dcounty.

[USGS] United States Geological Survey. 2021a. USGS 02299230 Myakka River at North Port Charlotte FL [dataset; accessed 2022 Apr 11]. https://waterdata.usgs.gov/nwis/inventory?agency_code=USGS&site_no=02299230.

[USGS] United States Geological Survey. 2021b. USGS 02297460 Peace River at Harbour Heights FL [dataset; accessed 2022 Apr 11]. https://waterdata.usgs.gov/nwis/inventory?agency_code=USGS&site_no=02297460.

Vellinga NE, Hoitink AJF, van der Vegt M, Zhang W, Hoekstra P. 2014. Human impacts on tides overwhelm the effect of sea level rise on extreme water levels in the Rhine–Meuse delta. Coastal Engineering. 90:40–50.

https://doi.org/10.1016/j.coastaleng.2014.04.005.

Wan Y, Ji Z-G, Shen J, Hu G, Sun D. 2012. Three dimensional water quality modeling of a shallow subtropical estuary. Marine Environmental Research. 82:76–86. https://doi.org/10.1016/j.marenvres.2012.09.007.

Weather Spark. 2023. Climate and average weather year round in Punta Gorda. [accessed 2023 Mar 10]. https://weatherspark.com/y/16793/Average-Weather-in-Punta-Gorda-Florida-United-States-Year-Round#Figures-WindSpeed.

Weishar LL, Teal JM, Hinkle R. 2005. Designing large-scale wetland restoration for Delaware Bay. Ecological Engineering. 25(3):231–239. https://doi.org/10.1016/j.ecoleng.2005.04.012.

Widdows J, Brinsley MD, Bowley N, Barrett C. 1998. A benthic annular flume for in situ measurement of suspension feeding/biodeposition rates and erosion potential of intertidal cohesive sediments. Estuarine, Coastal and Shelf Science. 46(1):27–38. https://doi.org/10.1006/ecss.1997.0259.

Wolanski E, Elliott M. 2015. Estuarine ecohydrology: an introduction. Kidlington, The Netherlands: Elsevier Science & Technology. https://doi.org/10.1016/C2013-0-13014-0.

Wolanski E, King B, Galloway D. 1995. Dynamics of the turbidity maximum in the Fly River estuary, Papua New Guinea. Estuarine, Coastal and Shelf Science. 40(3):321–337. https://doi.org/10.1016/S0272-7714(05)80013-7.

Yang Z, Khangaonkar T, Calvi M, Nelson K. 2010. Simulation of cumulative effects of nearshore restoration projects on estuarine hydrodynamics. Ecological Modelling. 221(7):969–977. https://doi.org/10.1016/j.ecolmodel.2008.12.006.

Yentsch CS, Lapointe BE, Poulton N, Phinney DA. 2008. Anatomy of a red tide bloom off the southwest coast of Florida. Harmful Algae. 7(6):817–826. https://doi.org/10.1016/j.hal.2008.04.008.

Zheng L, Weisberg RH. 2004. Tide, buoyancy, and wind-driven circulation of the Charlotte Harbor estuary: a model study. Journal of Geophysical Research: Oceans. 109(C6). https://doi.org/10.1029/2003JC001996.

JEED_Kramer_Arias_Peer_Review_File_060523.pdf 484 KB

References

- [CHNEP] Coastal and Heartland National Estuary Partnership. 2021. Charlotte Harbor Estuaries volunteer water quality monitoring network [database; accessed 2022 Apr 10]. https://chnep.wateratlas.usf.edu/chevwqmn/.

↩

↩

- [FDEP] Florida Department of Environmental Protection. 2005. Water quality assessment report–Charlotte Harbor. FDEP Division of Water Resource Management. [accessed 2022 Feb 1]. http://sarasota.wateratlas.usf.edu/upload/documents/Water%20Quality%20Assessment%20Report%20for%20the%20Charlotte%20Harbor%20Basin.pdf.

↩

- [FDEP] Florida Department of Environmental Protection. 2021. Gasparilla Sound–Charlotte Harbor Aquatic Preserve; [accessed 2021 Dec 30]. https://floridadep.gov/rcp/aquatic-preserve/locations/gasparilla-sound-charlotte-harbor-aquatic-preserve.

↩

- [NOAA NCEI] National Oceanic and Atmospheric Association National Centers for Environmental Information. 2021. Coastal relief model (3-second resolution) [dataset; accessed 2021 May 18]. National Oceanic and Atmospheric Association. https://www.ncei.noaa.gov/maps/grid-extract/.

↩

- [NOAA NCEI] National Oceanic and Atmospheric Association National Centers for Environmental Information. 2023. Climate at a glance county time series [dataset; accessed 2023 Mar 13]. https://www.ncei.noaa.gov/access/monitoring/climate-at-a-glance/county/time-series.

↩

- [NOAA] National Oceanic and Atmospheric Association. 2021a. Fort Myers, FL meteorological observations [dataset; accessed 2022 Apr 12]. NOAA Tides and Currents. https://tidesandcurrents.noaa.gov/met.html?id=8725520.

↩

- [NOAA] National Oceanic and Atmospheric Association. 2021b. Sea level rise viewer. NOAA Office for Coastal Management. [accessed 2022 Feb 7]. https://coast.noaa.gov/slr/.

↩

- [NOAA] National Oceanic and Atmospheric Association. 2022. Tropical cyclone report: Hurricane Elsa. National Hurricane Center. [accessed 2023 Mar 10]. https://www.nhc.noaa.gov/data/tcr/AL052021_Elsa.pdf.

↩

- [SWFWMD] Southwest Florida Water Management District. 2023. Environmental data portal | water data viewer: ROMP TR 3-1 Suwannee [dataset]; [accessed 2023 Mar 10]. https://edp.swfwmd.state.fl.us/applications/login.html?publicuser=Guest#waterdata-external/stationoverview.

↩

↩

- [USDA] United States Department of Agriculture. 1974. Aerial photographs of Charlotte County – Flight 274 (1974) [image; accessed 2023 May 24]. https://original-ufdc.uflib.ufl.edu/UF00071733/00028/8x?search=charlotte+%3dcounty.

↩

- [USGS] United States Geological Survey. 2021a. USGS 02299230 Myakka River at North Port Charlotte FL [dataset; accessed 2022 Apr 11]. https://waterdata.usgs.gov/nwis/inventory?agency_code=USGS&site_no=02299230.

↩

- [USGS] United States Geological Survey. 2021b. USGS 02297460 Peace River at Harbour Heights FL [dataset; accessed 2022 Apr 11]. https://waterdata.usgs.gov/nwis/inventory?agency_code=USGS&site_no=02297460.

↩

- Aretxabaleta AL, Butman B, Ganju NK. 2014. Water level response in back-barrier bays unchanged following Hurricane Sandy. Geophysical Research Letters. 41(9):3163–3171. https://doi.org/10.1002/2014GL059957.

↩

- Atkins Engineering. 2020. Manchester Waterway bathymetry pre- and post-dredging [unpublished dataset]. Atkins Engineers, Inc.

↩

- Bastidas LA, Knighton J, Kline SW. 2016. Parameter sensitivity and uncertainty analysis for a storm surge and wave model. Natural Hazards and Earth System Sciences. 16(10):2195–2210. https://doi.org/10.5194/nhess-16-2195-2016.

↩

- Brown S, Nicholls RJ, Woodroffe CD, Hanson S, Hinkel J, Kebede AS, Neumann B, Vafeidis AT. 2013. Sea-level rise impacts and responses: a global perspective. In: Finkl CW, editor. Coastal hazards. Dordrecht: Springer Netherlands. (Coastal Research Library). p. 117–149. [accessed 2022 Aug 25]. https://doi.org/10.1007/978-94-007-5234-4_5.

↩

- Chen X. 2020. Hydrodynamic simulations of Charlotte Harbor and its major tributaries in Florida using a dynamically coupled 3D–2DV model. Estuarine, Coastal and Shelf Science. 246. https://doi.org/10.1016/j.ecss.2020.107026.

↩

- Deltares. 2021. Delft3D-FLOW User Manual. Deltares. https://content.oss.deltares.nl/delft3d4/Delft3D-FLOW_User_Manual.pdf.

↩

- Earle S. 2019. Physical geology. 2nd ed. BCcampus. Chapter 13.3, Stream erosion and deposition. [accessed 2023 Mar 13]. https://opentextbc.ca/physicalgeology2ed/chapter/13-3-stream-erosion-and-deposition/.

↩

- Elliott M, Mander L, Mazik K, Simenstad C, Valesini F, Whitfield A, Wolanski E. 2016. Ecoengineering with ecohydrology: Successes and failures in estuarine restoration. Estuarine, Coastal and Shelf Science. 176:12–35. https://doi.org/10.1016/j.ecss.2016.04.003.

↩

- Florida State Parks. 2022. Charlotte Harbor Preserve State Park. [accessed 2022 Feb 1]. https://www.floridastateparks.org/parks-and-trails/charlotte-harbor-preserve-state-park.

↩

- George DA, Gelfenbaum G, Stevens AW. 2012. Modeling the hydrodynamic and morphologic response of an estuary restoration. Estuaries and Coasts. 35(6):1510–1529. https://doi.org/10.1007/s12237-012-9541-8.

↩

- Gobler CJ, Young CS, Goleski J, Stevens A, Thickman J, Wallace RB, Curran P, Koch F, Kang Y, Lusty MW, et al. 2019. Accidental ecosystem restoration? Assessing the estuary-wide impacts of a new ocean inlet created by Hurricane Sandy. Estuarine, Coastal and Shelf Science. 221:132–146. https://doi.org/10.1016/j.ecss.2019.02.040.

↩

- Google Earth Pro (7.3.6.9345). 2022 Apr 15. Charlotte Harbor, Florida Imagery, 26.9634657,-82.1674623. Image Landsat/Copernicus, Image © 2023 Maxar Technologies [accessed 2023 May 31]. https://earth.google.com/web/@26.9583937,-82.0670333,6622.97873637a,0d,35y,0h,0t,0r?utm_source=earth7&utm_campaign=vine&hl=en.

↩

- Green RH, Lowe RJ, Buckley ML. 2018. Hydrodynamics of a tidally forced coral reef atoll. Journal of Geophysical Research: Oceans. 123(10):7084–7101. https://doi.org/10.1029/2018JC013946.

↩

- Jay DA, Leffler K, Degens S. 2011. Long-term evolution of Columbia River tides. Journal of Waterway, Port, Coastal, and Ocean Engineering. 137(4):182–191. https://doi.org/10.1061/(ASCE)WW.1943-

↩

- Jiang Y, Wang Y, Zhou D, Ke Y, Bai J, Li W, Yan J. 2021. The impact assessment of hydro-biological connectivity changes on the estuary wetland through the ecological restoration project in the Yellow River Delta, China. Science of The Total Environment. 758:143706. https://doi.org/10.1016/j.scitotenv.2020.143706.

↩

- Jones HP, Hole DG, Zavaleta ES. 2012. Harnessing nature to help people adapt to climate change. Nature Climate Change. 2(7):504–509. https://doi.org/10.1038/nclimate1463.

↩

- Khojasteh D, Glamore W, Heimhuber V, Felder S. 2021. Sea level rise impacts on estuarine dynamics: A review. Science of The Total Environment. 780:146470. https://doi.org/10.1016/j.scitotenv.2021.146470.

↩

- Kim T, Peter Sheng Y, Park K. 2010. Modeling water quality and hypoxia dynamics in Upper Charlotte Harbor, Florida, U.S.A. during 2000. Estuarine, Coastal and Shelf Science. 90(4):250–263. https://doi.org/10.1016/j.ecss.2010.09.006.

↩

- Kulp SA, Strauss BH. 2019. New elevation data triple estimates of global vulnerability to sea-level rise and coastal flooding. Nat Commun. 10(1):4844. https://doi.org/10.1038/s41467-019-12808-z.

↩

- Leonard GH, Levine JM, Schmidt PR, Bertness MD. 1998. Flow-driven variation in intertidal community structure in a Maine estuary. Ecology. 79(4):1395–1411. https://doi.org/10.1890/0012-9658(1998)079%5b1395:FDVIIC%5d2.0.CO;2.

↩

- Liu Y, Weisberg RH, Zheng L. 2020. Impacts of Hurricane Irma on the circulation and transport in Florida Bay and the Charlotte Harbor Estuary. Estuaries and Coasts. 43(5):1194–1216. https://doi.org/10.1007/s12237-019-00647-6.

↩

- Manchester Waterway Civic Association. 2021. History of Manchester Waterway. Manchester Waterway Civic Association. [accessed 2023 Mar 8]. https://manchesterwaterway.org/manchester-waterway.

↩

- McLusky DS, Elliott M. 2004. The estuarine ecosystem: ecology, threats and management. 3rd ed. New York (NY): Oxford University Press U.S.A. ISBN: 9780198525080.

↩

- Naval Research Laboratory. 2022. HYCOM + NCODA Gulf of Mexico [dataset; accessed 2022 Apr 10]. https://www.hycom.org/data/gomu0pt04/expt-90pt1m000.

↩

- Pasch RJ, Reinhart BJ, Berg R, Roberts DP. 2021 National Hurricane Center tropical cyclone report: Hurricane Eta. National Hurricane Center. [accessed 2023 Mar 10]. https://www.nhc.noaa.gov/data/tcr/AL292020_Eta.pdf.

↩

- Passeri DL, Hagen SC, Plant NG, Bilskie MV, Medeiros SC, Alizad K. 2016. Tidal hydrodynamics under future sea level rise and coastal morphology in the Northern Gulf of Mexico. Earth's Future. 4(5):159–176. https://doi.org/10.1002/2015EF000332.

↩

- Prosser DJ, Jordan TE, Nagel JL, Seitz RD, Weller DE, Whigham DF. 2018. Impacts of coastal land use and shoreline armoring on estuarine ecosystems: an introduction to a special issue. Estuaries and Coasts. 41(1):2–18. https://doi.org/10.1007/s12237-017-0331-1.

↩

- Ralston DK, Talke S, Geyer WR, Al-Zubaidi HAM, Sommerfield CK. 2019. Bigger tides, less flooding: effects of dredging on barotropic dynamics in a highly modified estuary. Journal of Geophysical Research: Oceans. 124(1):196–211. https://doi.org/10.1029/2018JC014313.

↩

- Rangel-Buitrago N, Williams AT, Anfuso G. 2018. Hard protection structures as a principal coastal erosion management strategy along the Caribbean coast of Colombia. A chronicle of pitfalls. Ocean & Coastal Management. 156:58–75. https://doi.org/10.1016/j.ocecoaman.2017.04.006.

↩

- Silver JM, Arkema KK, Griffin RM, Lashley B, Lemay M, Maldonado S, Moultrie SH, Ruckelshaus M, Schill S, Thomas A, et al. 2019. Advancing coastal risk reduction science and implementation by accounting for climate, ecosystems, and people. Frontiers in Marine Science. 6. https://doi.org/10.3389/fmars.2019.00556.

↩

- Simms MJ. 2023. Tortoises, hares and the evolution of the Irish landscape. Geology Today. 39(1):13–17. https://doi.org/10.1111/gto.12416.

↩

↩

- Stark J, Plancke Y, Ides S, Meire P, Temmerman S. 2016. Coastal flood protection by a combined nature-based and engineering approach: modeling the effects of marsh geometry and surrounding dikes. Estuarine, Coastal and Shelf Science. 175:34–45. https://doi.org/10.1016/j.ecss.2016.03.027.

↩

- Stark J, Smolders S, Meire P, Temmerman S. 2017. Impact of intertidal area characteristics on estuarine tidal hydrodynamics: a modelling study for the Scheldt Estuary. Estuarine, Coastal and Shelf Science. 198:138–155. https://doi.org/10.1016/j.ecss.2017.09.004.

↩

- Vellinga NE, Hoitink AJF, van der Vegt M, Zhang W, Hoekstra P. 2014. Human impacts on tides overwhelm the effect of sea level rise on extreme water levels in the Rhine–Meuse delta. Coastal Engineering. 90:40–50. https://doi.org/10.1016/j.coastaleng.2014.04.005.

↩

- Wan Y, Ji Z-G, Shen J, Hu G, Sun D. 2012. Three dimensional water quality modeling of a shallow subtropical estuary. Marine Environmental Research. 82:76–86. https://doi.org/10.1016/j.marenvres.2012.09.007.

↩

- Weather Spark. 2023. Climate and average weather year round in Punta Gorda. [accessed 2023 Mar 10]. https://weatherspark.com/y/16793/Average-Weather-in-Punta-Gorda-Florida-United-States-Year-Round#Figures-WindSpeed.

↩

- Weishar LL, Teal JM, Hinkle R. 2005. Designing large-scale wetland restoration for Delaware Bay. Ecological Engineering. 25(3):231–239. https://doi.org/10.1016/j.ecoleng.2005.04.012.

↩

- Widdows J, Brinsley MD, Bowley N, Barrett C. 1998. A benthic annular flume for in situ measurement of suspension feeding/biodeposition rates and erosion potential of intertidal cohesive sediments. Estuarine, Coastal and Shelf Science. 46(1):27–38. https://doi.org/10.1006/ecss.1997.0259.

↩

- Wolanski E, Elliott M. 2015. Estuarine ecohydrology: an introduction. Kidlington, The Netherlands: Elsevier Science & Technology. https://doi.org/10.1016/C2013-0-13014-0.

↩

-

↩

- Yang Z, Khangaonkar T, Calvi M, Nelson K. 2010. Simulation of cumulative effects of nearshore restoration projects on estuarine hydrodynamics. Ecological Modelling. 221(7):969–977. https://doi.org/10.1016/j.ecolmodel.2008.12.006.

↩

- Yentsch CS, Lapointe BE, Poulton N, Phinney DA. 2008. Anatomy of a red tide bloom off the southwest coast of Florida. Harmful Algae. 7(6):817–826. https://doi.org/10.1016/j.hal.2008.04.008.

↩

- Zheng L, Weisberg RH. 2004. Tide, buoyancy, and wind-driven circulation of the Charlotte Harbor estuary: a model study. Journal of Geophysical Research: Oceans. 109(C6). https://doi.org/10.1029/2003JC001996.

↩